

# Development and application of the GenoBaits WheatSNP16K array to accelerate wheat genetic research and breeding

Shengjie Liu<sup>1,6</sup>, Mingjie Xiang<sup>2,6</sup>, Xiaoting Wang<sup>2,6</sup>, Jiaqi Li<sup>1</sup>, Xiangrui Cheng<sup>1</sup>, Huaizhou Li<sup>2</sup>, Ravi P. Singh<sup>3,4</sup>, Sridhar Bhavani<sup>3</sup>, Shuo Huang<sup>5</sup>, Weijun Zheng<sup>2</sup>, Chunlian Li<sup>2</sup>, Fengping Yuan<sup>1</sup>, Jianhui Wu<sup>2</sup>, Dejun Han<sup>2,\*</sup>, Zhensheng Kang<sup>1,\*</sup> and Qingdong Zeng<sup>1,\*</sup>

<sup>1</sup>State Key Laboratory for Crop Stress Resistance and High-Efficiency Production, College of Plant Protection, Northwest A&F University, Yangling 712100, Shaanxi, China

<sup>2</sup>State Key Laboratory for Crop Stress Resistance and High-Efficiency Production, College of Agronomy, Northwest A&F University, Yangling 712100, Shaanxi, China

<sup>3</sup>International Maize and Wheat Improvement Center (CIMMYT), El Batán, Texcoco, Estado de México 56237, Mexico

<sup>4</sup>Hubei Hongshan Laboratory, National Key Laboratory of Crop Genetic Improvement, College of Plant Science and Technology, Huazhong Agricultural University, No. 1 Shizishan Street, Hongshan District, Wuhan 430070, Hubei, China

<sup>5</sup>Key Laboratory of Plant Design, Chinese Academy of Sciences, CAS Center for Excellence in Molecular Plant Sciences, Shanghai Institute of Plant Physiology and Ecology, Chinese Academy of Sciences, Shanghai 200000, China

<sup>6</sup>These authors contributed equally to this article.

\*Correspondence: Dejun Han ([handj@nwafu.edu.cn](mailto:handj@nwafu.edu.cn)), Zhensheng Kang ([kangzs@nwsuaf.edu.cn](mailto:kangzs@nwsuaf.edu.cn)), Qingdong Zeng ([zengqd@nwafu.edu.cn](mailto:zengqd@nwafu.edu.cn))

<https://doi.org/10.1016/j.xplc.2024.101138>

## ABSTRACT

Single-nucleotide polymorphisms (SNPs) are widely used as molecular markers for constructing genetic linkage maps in wheat. Compared with available SNP-based genotyping platforms, a genotyping by target sequencing (GBTS) system with capture-in-solution (liquid chip) technology has become the favored genotyping technology because it is less demanding and more cost effective, flexible, and user-friendly. In this study, a new GenoBaits WheatSNP16K (GBW16K) GBTS array was designed using datasets generated by the wheat 660K SNP array and resequencing platforms in our previous studies. The GBW16K array contains 14 868 target SNP regions that are evenly distributed across the wheat genome, and 37 669 SNPs in these regions can be identified in a diversity panel consisting of 239 wheat accessions from around the world. Principal component and neighbor-joining analyses using the called SNPs are consistent with the pedigree information and geographic distributions or ecological environments of the accessions. For the GBW16K marker panel, the average genetic diversity among the 239 accessions is 0.270, which is sufficient for linkage map construction and preliminary mapping of targeted genes or quantitative trait loci (QTLs). A genetic linkage map, constructed using the GBW16K array-based genotyping of a recombinant inbred line population derived from a cross of the CIMMYT wheat line Yaco“S” and the Chinese landrace Mingxian169, enables the identification of *Yr27*, *Yr30*, and *QYr.nwafu-2BL.4* for adult-plant resistance to stripe rust from Yaco“S” and of *Yr18* from Mingxian169. *QYr.nwafu-2BL.4* is different from any previously reported gene/QTL. Three haplotypes and six candidate genes have been identified for *QYr.nwafu-2BL.4* on the basis of haplotype analysis, micro-collinearity, gene annotation, RNA sequencing, and SNP data. This array provides a new tool for wheat genetic analysis and breeding studies and for achieving durable control of wheat stripe rust.

**Key words:** wheat, liquid array, genotyping by target sequencing, stripe rust, resistance gene

Liu S., Xiang M., Wang X., Li J., Cheng X., Li H., Singh R.P., Bhavani S., Huang S., Zheng W., Li C., Yuan F., Wu J., Han D., Kang Z., and Zeng Q. (2025). Development and application of the GenoBaits WheatSNP16K array to accelerate wheat genetic research and breeding. *Plant Comm.* 6, 101138.

## INTRODUCTION

It is estimated that at least 56% more food than is currently produced will be required to meet the demand of the increasing world population by 2050 (van Dijk et al., 2021). Bread wheat (*Triticum aestivum*) is one of the most important crops that provide daily food and energy intake for humans globally. Breeding new wheat varieties with high and stable yields in a sustainable, environmentally friendly, and cost-effective way to meet these needs is a huge challenge (Grassini et al., 2013). Lack of germplasm with novel traits/genes is widely recognized as a limiting factor for the development of new high-yielding varieties, particularly in response to changing biotic and abiotic stresses, as the current level of genetic diversity available to wheat breeders has sharply declined owing to domestication and selection for yield under current agronomic management (Haudry et al., 2007; Tian et al., 2021). Despite the presence of thousands of accessions in gene banks and institutional collections, it is difficult to choose individual lines that will contribute to further improvement of modern cultivars owing to a lack of phenotypic and genotypic detail, particularly regarding so-called minor genes that ultimately contribute to final outcomes. Preliminary assessment of genetic diversity in germplasm using a set of genotypic data was necessary for separating core groups with potentially beneficial novel genes and quantitative trait loci (QTLs) for yield enhancement and subsequent in-depth studies (Kale et al., 2022; Schulthess et al., 2022). In the case of barley, 20 representative genotypes were selected for construction of chromosome-scale sequence assemblies from 23 000 barley accessions based on genotyping-by-sequencing (GBS) data (Jayakodi et al., 2020). In addition, genotypic data will facilitate the exchange of germplasm stored in gene banks and breeding institutions (Allen et al., 2017). Thus, to take full advantage of germplasm resources, a user-friendly genotyping platform for wheat is required for marker discovery.

Although *de novo* sequencing is the most anticipated way to comprehensively identify DNA variation in large germplasm collections (Walkowiak et al., 2020; Niu et al., 2023), it is not affordable for most research programs because of the large size of the wheat genome (International Wheat Genome Sequencing Consortium [IWGSC], 2018). Multiple cost-effective genotyping strategies such as exon sequencing, GBS, and solid high-density single-nucleotide polymorphism (SNP) arrays have been used to capture and identify large numbers of markers in wheat (He et al., 2019; Juliana et al., 2019; Pont et al., 2019; Wu et al., 2021). For example, development and application of the 15K, 35K, 50K, 55K, 90K, 660K, and 820K wheat arrays over the last decade have enabled the mining of germplasm, identification of genes/QTLs, and dissection of numerous important traits, especially those that are quantitatively controlled (Allen et al., 2017; Sun et al., 2020). However, genotyping using GBS or solid high-density SNP arrays has been limited by factors such as stability, reliability, specificity of the sequencing platforms, fixed SNP loci, and cost per sample (Guo et al., 2019, 2021). A new genotyping platform that overcomes these limitations is needed.

With significant progress in targeted sequencing and in-solution capture, a genotyping by target sequencing (GBTS) strategy has been developed whereby target genomic loci can be

captured by probes in liquid solution. GBTS combines the advantages of both GBS and solid-chip-based technologies. Target SNP loci in GBTS are flexible both in SNPs and samples, do not require special sequencing platforms, require less bioinformatics support, yield high accuracy, especially when genotyping genome-wide gene-based SNPs with high polymorphism and conserved flanking sequences, and are cost effective. GBTS can now be realized for small and large numbers of markers through multiplexing PCR (GenoPlexs) and capture-in-solution (liquid chip) with regular PCR plates (GenoBaits) (Xu et al., 2020). GBTS was first used in animals (Tewhey et al., 2009) and, in recent years, it has been successfully applied to crop plants such as maize (Guo et al., 2019), soybean (Liu et al., 2022c), and peanut (Sun et al., 2023). In maize, multiple affordable SNP marker arrays by GBTS have been developed for use in breeding. A multiple SNP (mSNP) calling process that can capture mSNPs from a single amplicon was also developed in maize by improvement of current GBTS systems and integration with capture-in-solution (liquid chip) (Guo et al., 2021). Compared with a one-amplicon-one-SNP system, mSNPs and within-mSNP haplotypes are more powerful for analysis of genetic diversity and linkage disequilibrium decay and for genome-wide association studies (GWASs).

Stripe rust, caused by the fungus *Puccinia striiformis* f. sp. *tritici* (*Pst*), is a significant challenge worldwide. Deployment of resistant varieties with durable adult-plant resistance (APR) apparently conferred by unique genes is now generally considered to be the best strategy for more comprehensive control of this and other diseases (Wellings, 2011; Ellis et al., 2014). To date, about 30 cataloged *Yr* genes (Chen and Kang 2017; Zhu et al., 2023) and more than 350 QTLs for APR to stripe rust have been identified in wheat or closely related species (Singh et al., 2022). However, most of these genes are currently underused by wheat breeders owing to individually minor effects and difficulties of selection based on phenotype. There is no doubt that reliable, breeder-friendly markers can assist with the accumulation of adequate resistance through combining (“stacking”) of targeted APR genes/QTLs using marker-assisted selection. For example, the development and deployment of the tightly linked marker *csSr2* for *Yr30/Lr27/Sr2/Pm70* (Mago et al., 2011a) and the gene-specific marker *cssfr1-6* for *Yr18/Lr34/Sr57Pm38* (Lagudah et al., 2009) have greatly improved selection efficiency (Ellis et al., 2014). Other advantages of some of these genes are their pleiotropic effects in conferring resistance to multiple diseases (Krattinger et al., 2009; Mago et al., 2011b) and their unique modes of action. Research on APR, including QTL mapping, fine mapping, map-based cloning, and GWASs supported by high-throughput genotyping to identify molecular markers tightly linked with, or ideally part of, target-trait genes, will continue in the future (Moore et al., 2015; Cobo et al., 2019; Juliana et al., 2019; Wu et al., 2021).

To promote wheat genetic research and improvement, the three objectives of this study were to: (1) identify a set of genome regions with high diversity distributed across the whole wheat genome using datasets generated by the wheat 660K SNP array and resequencing platforms in previous studies, then design a GenoBaits WheatSNP16K (GBW16K) array that specifically captures these regions; (2) validate the

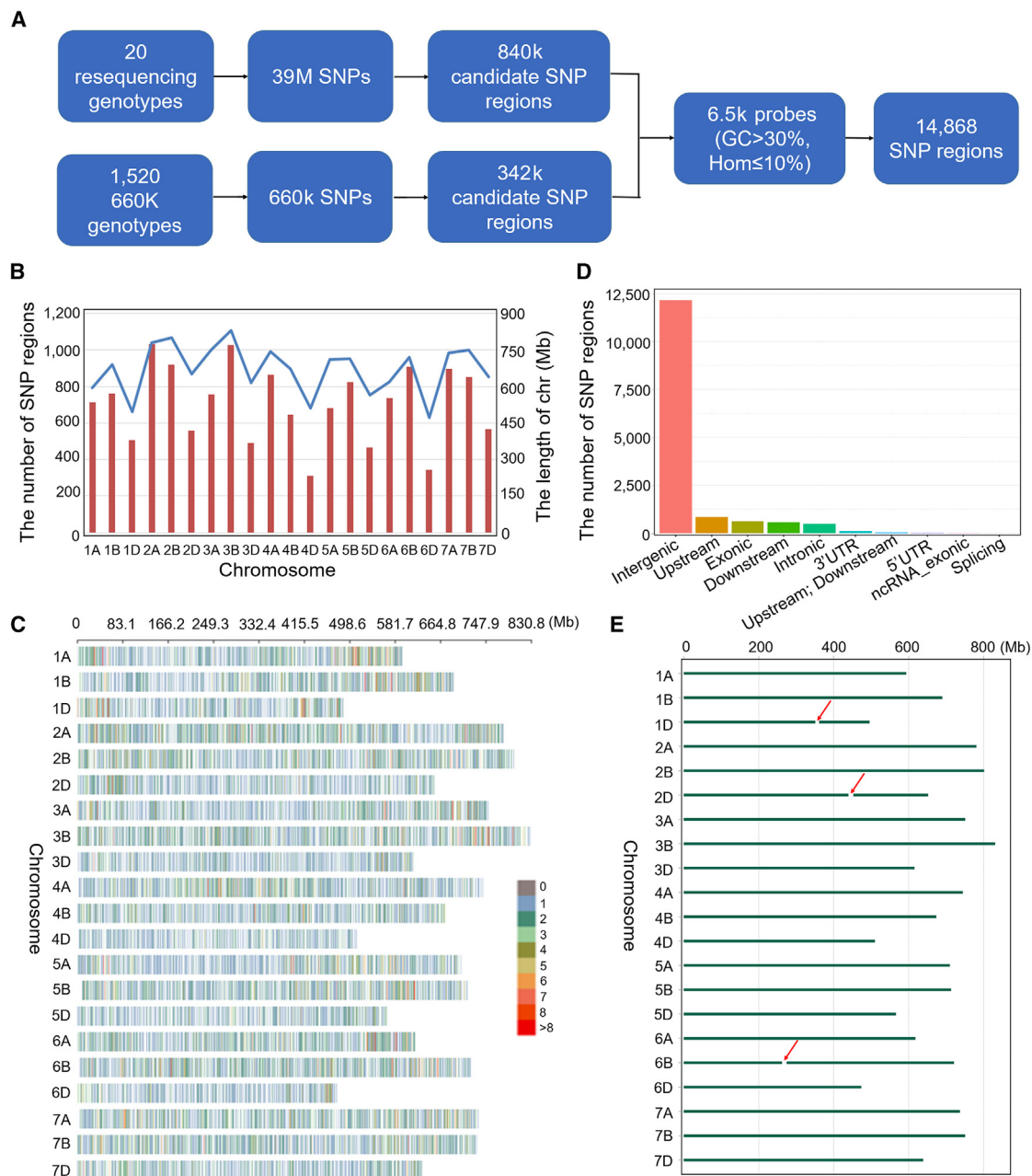


**Figure 1. Design and statistics of the GenoBaits Wheat16K (GBW16K) array.**

**(A)** Design pipeline of the GBW16K array.

**(B)** Number of target SNP regions on each chromosome. Blue line represents the length of individual chromosome.

**(C)** Density of the GBW16K array SNP regions in 1-Mb windows throughout the whole genome.

**(D)** Distribution of SNP regions within genome regions (intergenic, upstream, exonic, downstream, intronic, 3' UTR, 5' UTR, ncRNA\_exonic, and splicing).

**(E)** Positions of >5-Mb gaps in the genome. Red arrows indicate the locations of gaps.

utility of the GBW16K array for germplasm evaluation and high-resolution genetic linkage maps using a diverse bread wheat panel and a recombinant inbred line (RIL) population derived from a cross between the stripe rust resistant wheat Yaco“S” and the susceptible wheat Mingxian169 (MX169); and (3) determine the genetic basis of APR to stripe rust in Yaco“S” and map the relevant QTLs using a genetic linkage map developed from the RIL population.

## RESULTS

### Design and statistics of the GenoBaits WheatSNP16K array

The diversity of each SNP locus from the 660K array and resequencing datasets was analyzed to select appropriate genomic regions for target capture; 342k and 840k candidate genomic regions were identified from the 660K array and

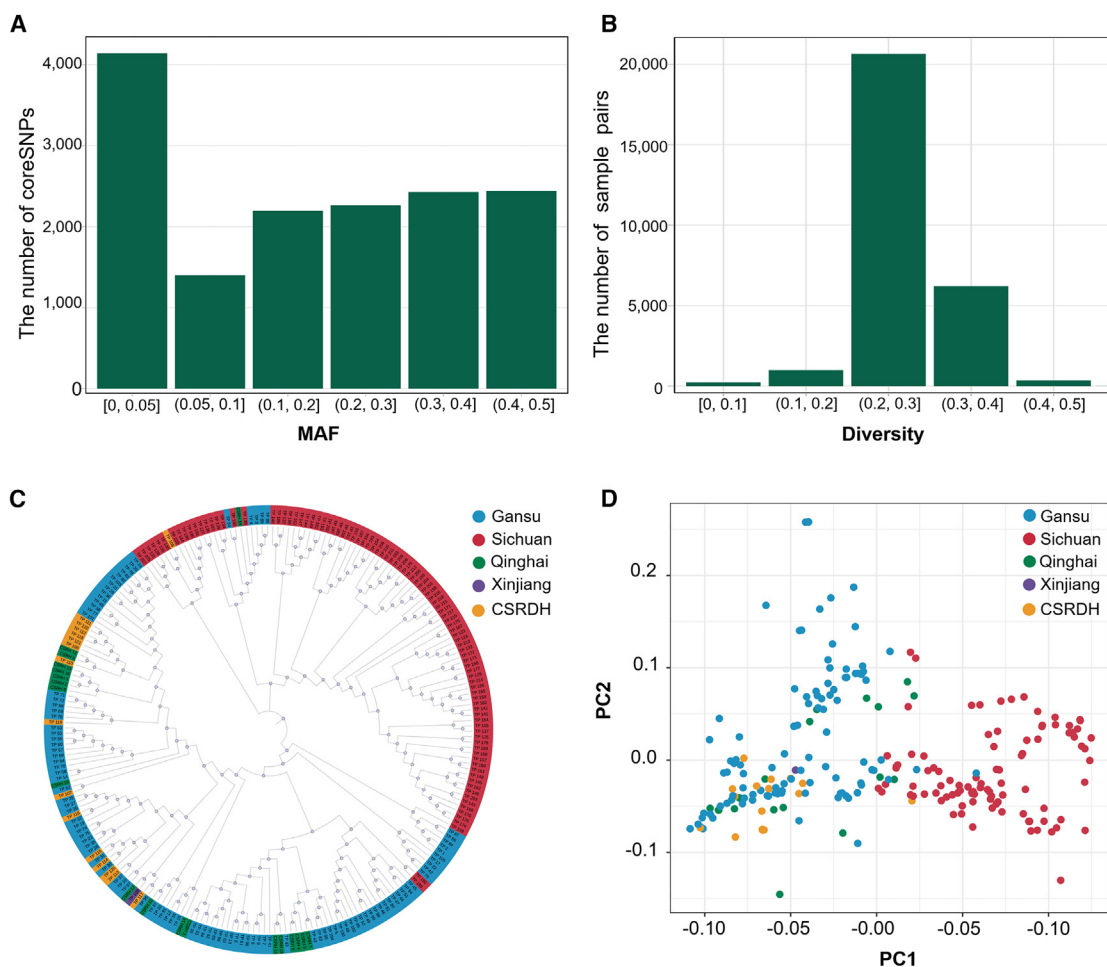


**Figure 2. Validation of the GBW16K array in 239 wheat accessions.**

(A) Minor allele frequency (MAF) distribution of the coreSNPs from each SNP region.

(B) Diversity distribution between any two wheat accessions based on mSNPs.

(C) Phylogenetic tree of accessions based on mSNPs. Each branch is color coded to represent accessions from distinct geographic regions.

(D) Principal coordinate analysis (PCoA) plots colored by geographic origin. Principal coordinate 1 is plotted along the x axis. Principal coordinate 2 is plotted along the y axis.

resequencing datasets, respectively. After a selection pipeline (Figure 1A), 4k bait probes were initially designed, and 10k genome regions were captured in a diversity panel of 239 accessions (Supplemental Table 1). An additional 2.5k bait probes to reduce the number of gap regions were designed from target candidate regions and tested on the same wheat panel (Figure 1A). Finally, 14 868 target-captured regions (each 110 nt in length) were obtained using all 6.5k probes (Supplemental Table 2). On the basis of GBW16K array genotype data for the 239 test wheat accessions, we called a total of 37 669 mSNPs, and the SNP with the highest minor allele frequency (MAF) in each region was defined as the “coreSNP” (Supplemental Table 2). To distinguish it from the wheat 15K SNP array, the GBTS liquid array was named the GenoBaits Wheat 16K SNP (GBW16K) array.

According to positions in the Chinese Spring (CS) reference genome IWGSC RefSeq v.1.0, the SNP regions almost uniformly covered the whole wheat genome (Figure 1B and 1C). The numbers of SNP regions across the 21 chromosomes

ranged from 313 (chromosome 4D) to 1030 (chromosome 2A) (Supplemental Table 3), averaging one region per 0.76 Mb (chromosome 2A) to 1.63 Mb (chromosome 4D). There were 12 160 (81.79%), 844 (5.68%), 609 (4.10%), 577 (3.88%), 493 (3.32%), and 185 (1.24%) SNP regions located in intergenic, upstream, exonic, downstream, intronic, and other genomic regions such as UTRs, respectively (Figure 1D and Supplemental Table 4). To further confirm the representativeness of the GBW16K array for wheat, each chromosome was divided into 1-Mb windows, and the numbers of SNP regions were counted in each window. Only three gaps >5 Mb on chromosomes 1D, 2D, and 6B were found in the GBW16K array (Figure 1E).

### Reproducibility of the GBW16K array

The reproducibility of a high-throughput genotyping platform is an important consideration for users. We tested the GBW16K array using the wheat cultivars Xinong 865 and Lantian 19 in three DNA duplicates to evaluate the target-capture efficiency. The call rates and genotypes of coreSNPs were highly similar and

Chr	Linkage group	No. of markers	Rate (%)	No. of bins	Length (cM)	Mean distance (cM/bin)	Density of markers (loci/cM)
1A	G1	633	6.84	163	266.67	1.64	2.37
2A	G4	439	4.75	135	237.35	1.76	1.85
3A	G7	551	5.96	126	283.84	2.25	1.94
4A	G10	1130	12.22	85	163.77	1.93	6.90
5A	G13 + G14	460	4.97	119	253.26	2.13	1.82
6A	G17	715	7.73	94	195.86	2.08	3.65
7A	G21	669	7.23	151	308.75	2.04	2.17
1B	G2	466	5.04	154	266.99	1.73	1.75
2B	G5	590	6.38	168	211.61	1.26	2.79
3B	G8	937	10.13	208	327.21	1.57	2.86
4B	G11	130	1.41	58	126.90	2.19	1.02
5B	G15	738	7.98	169	276.24	1.63	2.67
6B	G18 + G19	761	8.23	141	175.67	1.25	4.33
7B	G22 + G23	513	5.55	118	183.80	1.56	2.79
1D	G3	32	0.35	20	134.69	6.73	0.24
2D	G6	85	0.92	50	191.11	3.82	0.44
3D	G9	71	0.77	35	128.97	3.68	0.55
4D	G12	49	0.53	31	76.86	2.48	0.64
5D	G16	91	0.98	50	248.15	4.96	0.37
6D	G20	77	0.83	39	133.73	3.43	0.58
7D	G24 + G25	112	1.21	61	275.21	4.51	0.41
A genome	8	4597	49.70	873	1709.50	1.96	2.69
B genome	9	4135	44.72	1016	1568.42	1.54	2.64
D genome	8	517	5.59	286	1188.72	4.16	0.43
Total	25	9249	100.00	2175	4466.64	2.05	2.07

**Table 1. Marker statistics for distribution and density of SNPs on 21 wheat chromosomes.**

consistent across the DNA replicates. The call rate among duplicate samples ranged from 95.44% to 95.86% for Xinong 865 and from 95.30% to 95.76% for Lantian 19. The genotypic consistency ranged from 99.52% to 99.58% for Xinong 865 and from 99.47% to 99.58% for Lantian 19 (Supplemental Table 5). We also tested the GBW16K array using DNA from 10 wheat cultivars, including Xinong 865 and Lantian 19, in two batches to determine the effect of batch on genotype. The call rate among the 10 cultivars ranged from 97.22% to 99.28% in batch 1 and from 94.59% to 97.76% in batch 2. The genotypic consistency between the two batches ranged from 99.29% to 99.62% for the 10 cultivars (Supplemental Table 6). These results indicated the high reproducibility of the GBW16K array among samples and batches.

### Effectiveness of the GBW16K array in genetic research

Most of the coreSNPs called in 239 accessions had a large MAF (Figure 2A), indicating that these SNPs had high genetic diversity in the test population. Genetic diversity of markers among accessions is important for linkage map construction using data from biparental segregating populations. For the GBW16K array marker panel, the average genetic diversity among the

239 accessions was 0.270 (0.005–0.484) (Figure 2B and Supplemental Table 7). That is, when the GBW16K array is used to analyze a biparental population, it yields an average of 27% polymorphic markers. This corresponds to about 4k coreSNPs and 10k mSNPs, respectively. This marker density is sufficient for linkage map construction and preliminary mapping of any gene/QTL of interest.

Neighbor-joining (NJ) trees of the 239 accessions were constructed with the 37 669 mSNP genotypes. Two groups of genotypes were identified, one comprising materials from Sichuan province and the other including lines from Gansu, Qinghai, and Chinese stripe rust differential host (CSRDH) germplasms that are used to differentiate races of the wheat stripe rust pathogen in China (Figure 2C). The groups were confirmed by principal coordinate analysis (PCoA) plots (Figure 2D). The results of NJ trees and PCoA were consistent with the pedigree information and the locations where the cultivars were grown (Supplemental Table 1). The main wheat area in Sichuan province is in a basin with a subtropical humid monsoon climate that is very different from the arid to semi-arid plateau regions of Gansu and Qinghai. Moreover, the breeding programs in Sichuan are relatively independent of those in the adjacent

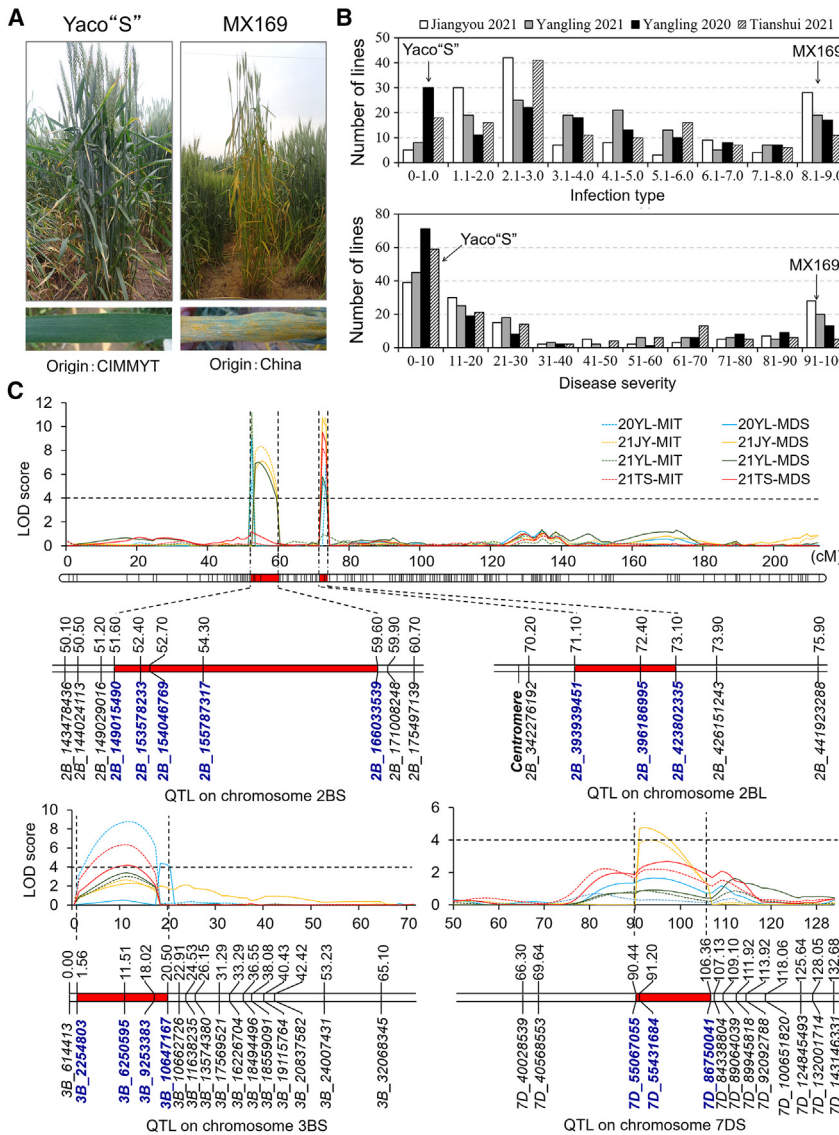


**Figure 3. Phenotypic and QTL analysis of stripe rust response in the Yaco'S' x MX169 RIL population.**

**(A)** Phenotypes of Yaco'S' and MX169 challenged with stripe rust at the adult-plant stage.

**(B)** Phenotypic distributions of mean infection types (IT) and disease severities (DS) for Yaco'S' x MX169 RILs across four environments. Values for the parents Yaco'S' and MX169 are indicated by arrows.

**(C)** Linkage maps and QTL mapping for three chromosome arms. QTLs were identified by inclusive composite interval mapping (ICIM). Confidence intervals of QTLs and markers significantly linked with QTLs are marked in red and blue, respectively. LOD score refers to the logarithm of odds score. YL, JY, and TS represent Yangling, Jiangyou, and Tianshui, and 20 and 21 represent the crop seasons of 2020 and 2021. MIT and MDS represent the mean IT and mean DS of all replicates in each environment.

(<https://isbreeding.caas.cn/rj/qtlmapping/294445.htm>); 272 SNPs were removed because they had >20% missing data or showed segregation distortion ( $p > 0.001$ ). Markers with the lowest rates of missing data in each bin were selected as bin markers for genetic map construction. A linkage map with 25 linkage groups representing all 21 chromosomes was constructed using the CS physical reference map. The entire map covered 4466.64 cM with an average marker/bin interval of 2.05 cM (Supplemental Figure 1 and Table 1).

To map the major QTLs in the resistant parent Yaco'S', the stripe rust responses of the RILs and parents were determined in multiple environments. Yaco'S' and MX169 showed stripe rust resistance (infection type [IT] = 0, disease severity [DS] = 0%) and susceptibility (IT = 9, DS > 90%), respectively, in the field, consistent with scores from a previous study (Figure 3A) (Li et al., 2017). The IT and DS data for the RILs were continuously distributed across the entire range of response, indicating that APR was polygenically inherited (Figure 3B). ANOVA indicated that lines and environments were the main determinants of phenotypic variation, with no significant variation among replicates within each environment ( $p < 0.001$ ). Broad-sense heritabilities were 0.92 for IT and 0.93 for DS (Supplemental Table 8). Pearson's correlation coefficients among the four environments ranged from 0.65 to 0.81 for IT and from 0.67 to 0.87 for DS (Supplemental Table 9). These results suggested that the APR in Yaco'S' was consistently effective across environments.

provinces of Gansu and Qinghai. Germplasm adapted to Gansu and Qinghai is frequently exchanged, and most cultivars grown in Qinghai were bred in Gansu. Although most CSRDH germplasms, such as Funo introduced from Italy in the 1950s, came from foreign countries, they clustered with the latter (Supplemental Table 1). It is worth noting that several Sichuan cultivars clustered with Gansu material, indicating that some exchange does occur because of the common problem of stripe rust. Overall, these results indicate that the GBW16K array is suitable for use in genetic studies and breeding involving diverse germplasms.

**A case of the GBW16K array used in QTL mapping**

To validate the effectiveness of the GBW16K array in gene/QTL mapping using a biparental population, 136 RILs and the Yaco'S' and MX169 parents were genotyped with the array to map loci that confer stripe rust resistance. A total of 9249 mSNPs were identified between the parents. These markers fell into 2175 bins for linkage group construction using the "BIN" function in IciMapping v.4.2

Four QTLs related to mean IT (MIT) and mean DS (MDS) on chromosome arms 2BS, 2BL, 3BS, and 7DS were detected by the inclusive composite interval mapping (ICIM) method (Figure 3C and Table 2); three were contributed by Yaco'S', whereas *QYr.nwafu-7DS* came from MX169. *QYr.nwafu-2BS*, a major

QTL, environment <sup>a</sup>	Flanking marker	Genetic position <sup>b</sup> (cM)	Physical position <sup>c</sup> (Mb)	LOD <sup>d</sup>	PVE <sup>e</sup>	ADD <sup>f</sup>
<b>QYr.nwafu-2BS (YrAc)</b>						
CYR34	2B_149015490-2B_153578233	52	149.0–153.6	6.5	22.2	–0.9
20YL-IT	2B_149015490-2B_153578233	52	149.0–153.6	5.5	13.3	–0.9
20YL-DS	2B_149015490-2B_153578233	52	149.0–153.6	9.1	25.6	–15.7
21JY-IT	2B_155787317-2B_166033539	55	155.8–166.0	8.3	20.0	–1.1
21JY-DS	2B_155787317-2B_166033539	55	155.8–166.0	7.1	16.9	–13.8
21YL-IT	2B_149015490-2B_153578233	52	149.0–153.6	11.2	27.5	–1.4
21YL-DS	2B_149015490-2B_153578233	54	149.0–153.6	7.0	22.5	–13.8
<b>QYr.nwafu-2BL.4 (novel)</b>						
20YL-IT	2B_396186995-2B_423802335	73	396.2–423.8	6.8	16.5	–1.0
20YL-DS	2B_393939451-2B_396186995	72	393.9–396.2	5.3	14.7	–11.6
21JY-IT	2B_393939451-2B_396186995	72	393.9–396.2	10.7	26.5	–1.2
21JY-DS	2B_393939451-2B_396186995	72	393.9–396.2	10.7	26.4	–16.6
21YL-DS	2B_393939451-2B_396186995	72	393.9–396.2	5.8	19.3	–12.4
21TS-IT	2B_393939451-2B_396186995	72	393.9–396.2	8.2	22.2	–1.2
21TS-DS	2B_393939451-2B_396186995	72	393.9–396.2	9.5	25.1	–16.3
<b>QYr.nwafu-3BS (Yr30)</b>						
20YL-IT	3B_6250595-3B_9253383	12	6.3–9.3	8.8	22.5	–1.1
20YL-DS	3B_9253365-3B_10647167	19	4.3–9.1	4.4	11.7	–10.3
21TS-IT	3B_6250595-3B_9253383	12	6.3–9.3	6.3	16.6	–1.0
21TS-DS	3B_6250595-3B_9253383	12	6.3–9.3	4.2	10.2	–10.3
<b>QYr.nwafu-7DS (Yr18)</b>						
21JY-IT	7D_55431684-7D_86750041	93	55.4–86.8	4.0	9.8	0.7
21JY-DS	7D_55431684-7D_86750041	92	55.4–86.8	4.8	10.8	10.5

**Table 2. Quantitative trait loci (QTLs) for stripe rust resistance detected in the Yaco“S” × MX169 RIL population using infection type and disease severity data from four environments.**

<sup>a</sup>YL and JY, Yangling and Jianguyou; 20 and 21, field experiments during 2019–2020 and 2020–2021.

<sup>b</sup>Genetic position of QTL on the genetic map (cM).

<sup>c</sup>Physical position of QTL in IWGSC RefSeq v.1.0 (Mb).

<sup>d</sup>LOD, logarithm of odds.

<sup>e</sup>PVE, percentage of phenotypic variance explained.

<sup>f</sup>ADD, additive effect.

QTL identified by bulked segregant analysis (BSA) in a previous study (Li et al., 2017), was detected in environments 20YL, 21JY, and 21YL, explaining 13.3%–27.5% of the phenotypic variation in IT and 16.9%–25.6% of the variation in DS. *QYr.nwafu-2BL.4*, mapped to a 2.0-cM interval flanked by SNP markers *2B\_393939451* and *2B\_423802335* in the centromere region of chromosome arm 2BL; it had a consistent effect across all environments and explained 16.5%–26.5% of the phenotypic variation in IT and 14.7%–26.4% of the variation in DS. *QYr.nwafu-3BS* and *QYr.nwafu-7DS* explained 9.8%–22.5% of the phenotypic variation in IT and 10.2%–11.7% of the variation in DS in only one or two environments.

### Fine-mapping the causal gene in *QYr.nwafu-2BS* using GBW16K and 660K arrays

Line YM106 identified from the F<sub>5</sub> RIL population segregated for plants showing near-immune (IT ≤ 1, DS ≤ 5%) and high-to-moderate resistance (IT = 3–4, DS = 10%–20%) responses. For

convenience, the groups were denoted later as R and S, respectively. A near-isogenic line (NIL) pair, YM106R/YM106S, and a YM106 F<sub>6</sub> population of 540 plants were inoculated with *Pst* race CYR34 at different growth stages. YM106S was susceptible (IT = 9) at all growth stages. YM106R was susceptible (IT = 9) at the two- and three-leaf stages but showed resistance from the four-leaf stage on, progressing to a fully immune response at the five-leaf and later stages (Figure 4A).

To determine which locus was responsible for the phenotypic difference between YM106R and YM106S, the two lines were genotyped with the GBW16K array, and 230 (2.5%) polymorphic SNPs were identified. The largest proportion of SNPs was in chromosome arm 2BS, indicating that the locus was *QYr.nwafu-2BS* (Figure 4B). According to the genotypes of flanking markers for the other QTLs, both YM106R and YM106S carried the other three QTLs. To verify this result, the YM106 F<sub>6</sub> population and derived F<sub>6:7</sub> lines were phenotyped for stripe rust response screening, and BSA was performed with the

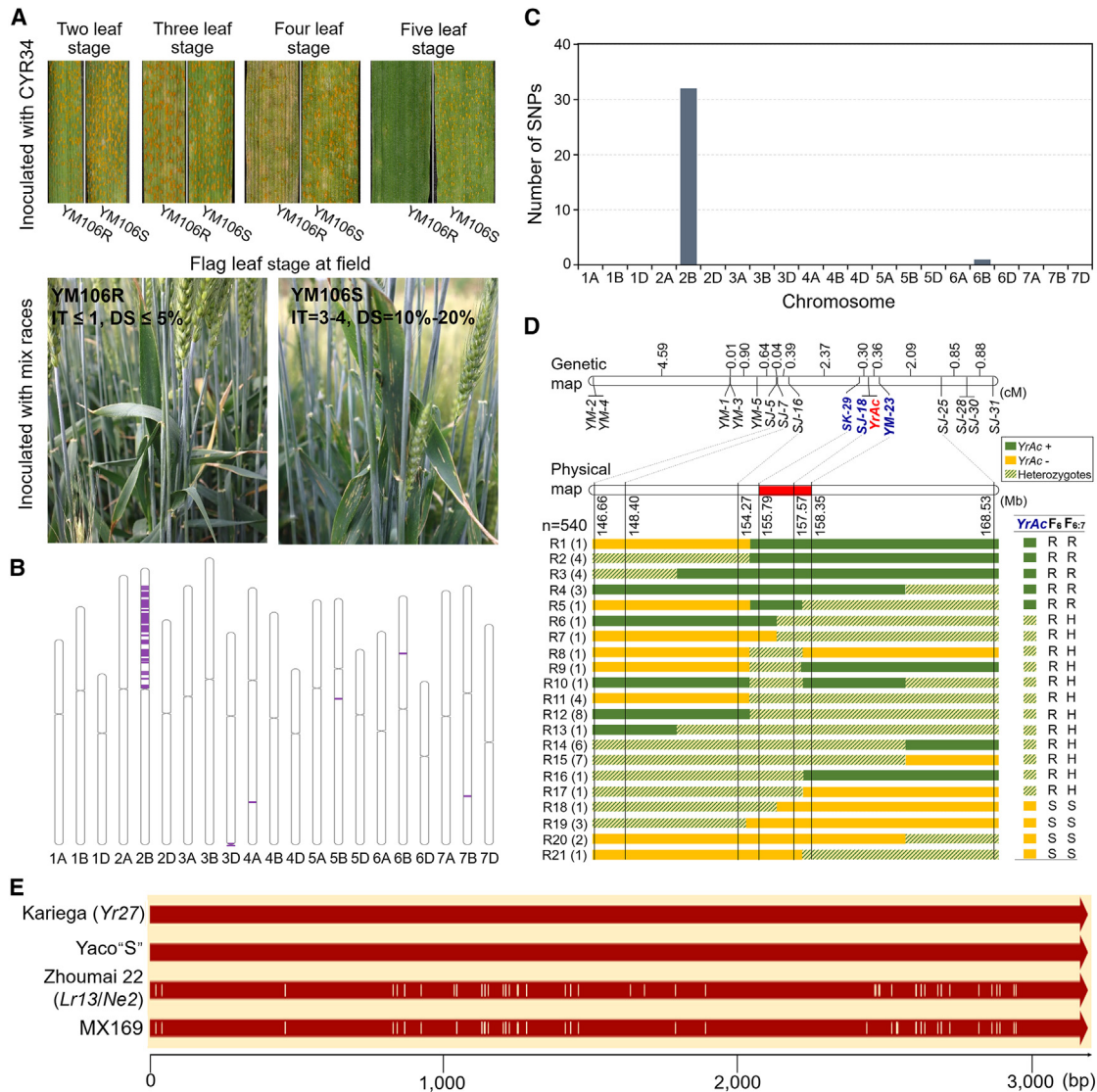


**Figure 4. Phenotypic responses of YM106R/YM106S NILs to stripe rust and fine mapping of *QYr.nwafu-2BS/YrAc*.**

**(A)** Upper: stripe rust responses of YM106R and YM106S at different developmental stages (two- to five-leaf stage). Observe the increasing resistance of YM106R. Lower: stripe rust responses of YM106R and YM106S in the field.

**(B)** Genetic differences (purple) between YM106R and YM106S based on the GBW16K array.

**(C)** Distribution of polymorphic SNPs across each chromosome. The SNPs were identified from bulked segregant analysis of stripe rust response in the YM106 F<sub>6</sub> population.

**(D)** High-resolution genetic and physical map of YrAc. The region in red marks the confidence interval of YrAc; markers significantly linked to QTLs are marked in red and blue. n indicates the number of lines used in mapping; R, S, and H denote homozygous resistant, homozygous susceptible, and heterozygous, respectively. R1–R21 represent different recombinant types. Numbers in parentheses represent the number of each recombinant type.

**(E)** Polymorphisms in the CDS of the candidate gene *TraesCS2B01G182800.1* among wheat cultivars Kariega (Yr27), Yaco“S”, Zhoumai 22 (*Lr13/Ne2*), and MX169. Red indicates nucleotide sequence consistency; beige indicates nucleotide sequence inconsistency.

GBW16K array. The F<sub>6</sub> population segregated into 398 resistant/142 susceptible individuals, fitting a 3:1 ratio ( $\chi^2 = 0.453$ ;  $p_{1df} > 0.05$ ) and suggesting that a dominant gene, provisionally designated YrAc, was involved. There were 33 SNPs between the R pool and S pool, and a candidate genomic region with 32 SNPs was identified on chromosome 2BS (Figure 4C). Fifteen competitive allele-specific PCR (KASP) markers (Supplemental Table 10), derived from 60 SNPs from the 660K genotyping data for Yaco“S” and MX169, were developed and used to genotype the 540 F<sub>6</sub> plants. A genetic map spanning 13.42 cM

was constructed using Joinmap v.4.0. YrAc co-segregated with KASP marker SJ-18 and was flanked by markers SK-29 and YM-23 at genetic distances of 0.30 cM and 0.36 cM, respectively (Figure 4D). In this region, a nucleotide-binding leucine-rich repeat (NLR) gene whose alleles with 97% similarity encoded Yr27 and *Lr13* was identified as a candidate causal gene from 20 high-confidence annotated genes in IWGSC RefSeq v.1.0 and v.2.1 on the basis of expression level and sequence variations in the parental lines (Supplemental Figure 2 and Supplemental Table 11) (Hewitt et al., 2021; Yan et al., 2021;

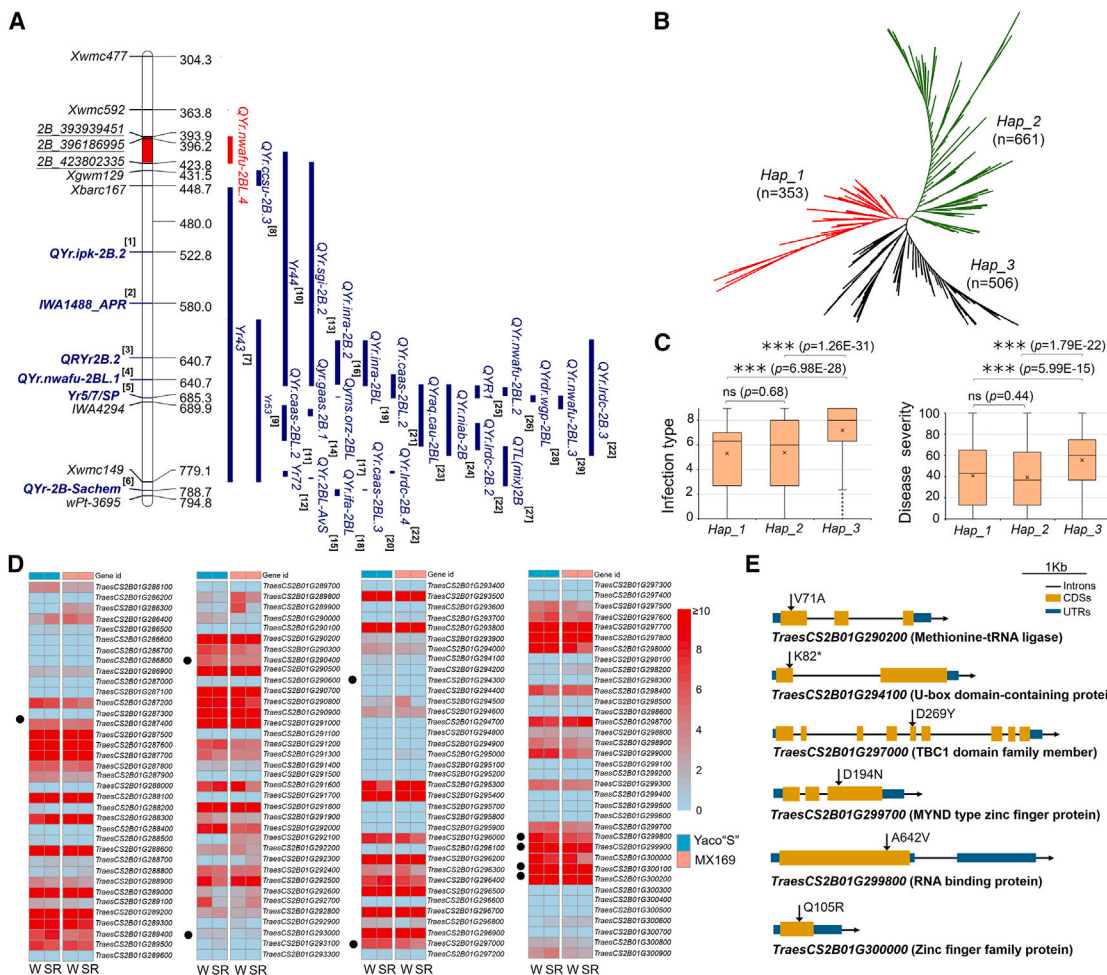


**Figure 5. Physical location, haplotype analysis, and candidate genes of *QYr.nwafu-2BL.4* in chromosome arm 2BL.**

(A) *QYr.nwafu-2BL.4* and previously mapped *Pst* resistance genes/QTLs are positioned on IWGSC RefSeq v.1.0. *QYr.nwafu-2BL.4* and reported genes/QTLs are marked in red and blue, respectively. Detailed information on genes/QTLs is provided in Supplemental Table 12. References: <sup>[1]</sup>Draz et al. (2021); <sup>[2]</sup>Zegeye et al. (2014); <sup>[3]</sup>Zhou et al. (2015); <sup>[4]</sup>Jighly et al. (2015); <sup>[5]</sup>Marchal et al. (2018); <sup>[6]</sup>Singh et al. (2013); <sup>[7]</sup>Cheng and Chen (2010); <sup>[8]</sup>Kumar et al. (2013); <sup>[9]</sup>Xu et al. (2013); <sup>[10]</sup>Sui et al. (2009); <sup>[11]</sup>Ren et al. (2012); <sup>[12]</sup>Chhetri et al. (2023); <sup>[13]</sup>Ramburan et al. (2004); <sup>[14]</sup>Cheng et al. (2022); <sup>[15]</sup>Rosewarne et al. (2008); <sup>[16]</sup>Mallard et al. (2005); <sup>[17]</sup>Vazquez et al. (2015); <sup>[18]</sup>Buerstmayr et al. (2014); <sup>[19]</sup>Pailard et al. (2012); <sup>[20]</sup>Liu et al. (2015); <sup>[21]</sup>Ren et al. (2015); <sup>[22]</sup>Farzand et al. (2021); <sup>[23]</sup>Guo et al. (2008); <sup>[24]</sup>Powell et al. (2013); <sup>[25]</sup>Boukhatem et al. (2002); <sup>[26]</sup>Zeng et al. (2019a); <sup>[27]</sup>Christiansen et al. (2006); <sup>[28]</sup>Hou et al. (2015); <sup>[29]</sup>Zeng et al. (2019b).

(B) Phylogenetic tree of the candidate *QYr.nwafu-2BL.4* region using 660K array data. *Hap\_1* (Yaco“S”), *Hap\_2* (MX169), and *Hap\_3* are found mainly in CIMMYT and ICARDA derivatives, landraces, and modern Chinese cultivars. Numbers of wheat accessions and their frequencies are listed alongside the corresponding haplotypes. Details of results based on 660K wheat SNP markers are available in Supplemental Table 13.

(C) Stripe rust responses of different haplotype groups in the field. ns, no significant difference. \*\*\**p* < 0.001 (Student’s *t*-test).

(D) Expression levels of high-confidence genes within the interval of *QYr.nwafu-2BL.4*. Black dots highlight nine genes with SNP mutations in the coding sequence between Yaco“S” and MX169. W, inoculated with water; SR, inoculated with stripe rust.

(E) Structures and positions of amino acid variations in the six candidate genes. Arrows indicate the locations of amino acid variations. Detailed information on the high-confidence genes is provided in Supplemental Table 14.

Athiyannan et al., 2022). Sanger sequencing and alignment of the coding sequences (CDSs) confirmed that YrAc was Yr27 and differed from the CDS in MX169 by 42 nucleotides and 27 amino acids (Figure 4E; Supplemental Figures 3 and 4).

**A focus on *QYr.nwafu-2BL.4***

To confirm the novelty of *QYr.nwafu-2BL.4*, we collected reported stripe rust resistance genes/QTLs on chromosome arm 2BL and mapped them in IWGSC RefSeq v.1.0 by blast using the DNA sequences of flanking markers (Supplemental

Table 12). Among the seven genes and 26 QTLs, most were located in the terminal region of arm 2BL and were more than 120 Mb distal to *QYr.nwafu-2BL.4*, with the exceptions of *QYr.ccsu-2B.3* in W7984 and *QYr.sgi-2B.1* in Kariega (Figure 5A). *QYr.ccsu-2B.3* was in the 431.48- to 448.71-Mb interval between markers *Xgwm129* and *Xbarc167* and 5 Mb proximal to *QYr.nwafu-2BL.4*. *QYr.ccsu-2B.3*, which accounted for 5.86%–10.96% of the phenotypic variance explained (PVE), was detected in only one of the four test environments compared with *QYr.nwafu-2BL.4*, which was identified as a major APR locus consistent across all environments

(Kumar et al., 2013). The difference in position and effect suggested that *QYr.ccsu-2B.3* and *QYr.nwafu-2BL.4* involved different genes. Considering all results, we concluded that *QYr.nwafu-2BL.4* was a novel gene for APR to stripe rust.

Using the 660K array genotypes, 1254 SNPs in 1520 wheat accessions were identified in the mapped interval for *QYr.nwafu-2BL.4* (Supplemental Table 13). There were three major haplotypes in this region, which were designated *Hap\_1* (23.22% of accessions), *Hap\_2* (43.49%), and *Hap\_3* (33.29%) (Figure 5B). Yaco“S” and MX169 belonged to *Hap\_1* and *Hap\_2*, respectively. The mean IT and DS for *Hap\_1* in three stripe rust test locations were significantly lower than those for *Hap\_3* but not *Hap\_2* ( $p < 0.001$ ), possibly owing to the presence of other unknown resistance genes (Figure 5C). *Hap\_1* accessions were mainly cultivars or breeding lines from the International Maize and Wheat Improvement Center (CIMMYT) and the International Center for Agricultural Research in the Dry Areas (ICARDA), whereas *Hap\_2* and *Hap\_3* consisted mainly of landraces and modern Chinese cultivars (Supplemental Table 13), suggesting that *QYr.nwafu-2BL.4* has not been selected in resistance breeding programs in China.

Micro-collinearity analysis using the TGT online tool showed that the 27-Mb genome region containing *QYr.nwafu-2BL.4* was largely conserved across Triticeae genomes (Supplemental Figure 5). The absence of insertions, deletions, and inversions gave confidence for predicting candidate genes for *QYr.nwafu-2BL.4*. There were 144 high-confidence genes in the interval according to the CS reference sequence IWGSC RefSeq v.1.0 and v.2.1 (Supplemental Table 14). Expression analyses of flag-leaf RNA-sequencing (RNA-seq) data for these genes in Yaco“S” and MX169 reduced the number of candidates to 89 genes expressed at different levels in Yaco“S” (Figure 5D and Supplemental Table 14). Fifteen SNPs between Yaco“S” and MX169 were detected in nine of 89 expressed genes (Figure 5D and Supplemental Table 14). Among them, *TraesCS2B01G294100*, which encodes a U-box domain-containing protein, carried a stop mutation in MX169. *TraesCS2B01G290200*, *TraesCS2B01G297000*, *TraesCS2B01G299700*, *TraesCS2B01G299800*, and *TraesCS2B01G300000*, which encode a methionine-tRNA ligase, a TBC1 domain family member, an MYND type zinc-finger protein, an RNA-binding protein, and a zinc-finger family protein, respectively, carried nonsense mutations (Figure 5E and Supplemental Table 14). These six genes were therefore identified as potential candidates for *QYr.nwafu-2BL.4* on the basis of gene annotation, RNA-seq, and SNP data. Further experiments including transgene and mutant analysis will be required to confirm the causal gene of *QYr.nwafu-2BL.4*.

To promote exploitation of *QYr.nwafu-2BL.4*, KASP markers AX-89538602 and AX-109506225 (Supplemental Table 10), which co-segregated with marker *2B\_396186995* and were most significantly correlated with stripe rust resistance in the RIL population, were developed from SNPs between Yaco“S” and MX169 in the 660K array. A validation study showed that AX-89538602 was polymorphic in the worldwide panel of 1520 wheat accessions (Supplemental Figure 6 and Supplemental Table 15), indicating that it has broad utility for molecular marker-assisted selection (MAS).

## DISCUSSION

### The GBW16K array and its application in wheat genetic research and breeding

In this study, we report a novel high-throughput genotyping platform, the GBW16K array, containing 14 868 target genome regions (Supplemental Table 2) and showing >99% reproducibility (Supplemental Tables 5 and 6), based on GBTS by target sequencing and liquid chip technology. The present array highlights the uniform distribution of markers across the genome and the diversity of markers (Figure 1). Only three gaps greater than 5 Mb (Figure 1E) and an average genetic diversity of 0.270 (Supplemental Table 7) were found between random pairs of wheat lines, making the array suitable for cost-efficient generation of genetic maps involving a range of parental lines, for genotyping wheat germplasm from a wide range of sources, and for background selection in wheat breeding. For example, the GBW16K array was used in a study of genetic diversity and kinship analysis of 239 wheat accessions (Figure 2), construction of a linkage map for the YM RIL population (Table 1 and Supplemental Figure 1), primary mapping (Figure 3C), evaluation of genetic background similarity between the NILs YM106R and YM106S (Figure 4B), and bulk segregant analysis for the major stripe rust resistance gene *Yr27* (Figure 4C).

The GBW16K array was used in recent wheat genetic studies. Qiao et al. (2021) identified genetic regions involved in determination of grain number per spike in the Chinese founder parent Linfen 5064 using a linkage map of 3045.86 cM constructed for a doubled haploid population. Huang et al. (2023) constructed a linkage map for an RIL population and found four stable APR QTLs for stripe rust resistance in the Chinese wheat cultivar Xinong 3517. The GBW16K array is also useful for research and breeding applications such as GWASs and genomic selection. GWASs of diverse wheat panels identified chromosome regions involved in determination of grain hardness and grain number (Zheng et al., 2021; Wang et al., 2022). Although the GBW16K array genotyping platform provides a new option for researchers and will contribute to wheat genetic studies and breeding, there may be difficulties in identifying causal genes owing to the relatively low marker density.

### Advantages of the GBW16K array compared with existing wheat arrays

When a new tool is developed, it is necessary to make comparisons with existing tools to clarify its advantages. We therefore compared the GBW16K array with the existing 15K, 35K, 50K, 55K, 90K, 660K, and 820K wheat arrays that were developed for genetic research and molecular breeding applications (Table 3) (Allen et al., 2017; Sun et al., 2020). The high-density 90K, 660K, and 820K arrays are suitable for wider application scenarios, including fine mapping and identification of causal genes controlling traits of interest (Allen et al., 2017). However, the high densities of their markers may incur a higher cost for genotyping each individual, thereby limiting the population size. More importantly, a high-density array is not necessary for many application scenarios, such as genetic background selection in MAS, linkage map construction, primary mapping of QTLs, and germplasm diversity assessment. Indeed,

Array name	Array type	Distribution of loci on genome	Main application scenarios	Sequencing platform	Detectable variation	Cost per sample	Integration of data from different programs
660K	Solid array	Whole genome	Linkage map construction and gene mapping or cloning, bulk segregant analysis, molecular marker-assisted selection, germplasm evaluation, genome selection, GWAS	Specific instrument	Known fixed SNP loci	High	Easy
820K							
90K							
55K							
35K							
15K	/	Random genome segments	Linkage map construction, gene primary mapping, bulk segregant analysis, molecular marker-assisted selection, germplasm evaluation, genome selection	All second generation and third generation	All variations in target region	Lower	Difficult
GBS							
GBW16K	Liquid array	Whole genome					Easy

**Table 3. Comparative analysis of the GBW16K array with GBS and existing wheat arrays.**

Red cells highlight the advantages of the GBW16K array compared with other wheat arrays.

the 15K, 35K (derived from 820K), 50K, and 55K (derived from 660K) arrays with lower-density markers were developed to reduce the genotyping cost of each sample to an affordable level.

The GBW16K array was developed with GBTS technology, combining the advantages of GBS and solid-chip technology for use in applications similar to those of the 15K, 35K, 50K, and 55K arrays but achieving more flexibility and cost-effectiveness in three ways (Table 3). First, existing wheat arrays are based on the solid array method, with genotyping performed by specific sequencing platforms, but the GBW16K array can be genotyped by any sequencing platform that is available to users. Second, the existing wheat arrays can detect only a known, fixed number of SNP loci, but the GBW16K array can detect both sample-specific and unknown variations in target loci, enabling identification of more genetic variation that may be important for genetic studies. For example, we obtained 37 669 mSNPs, many more than the 14 868 loci used in the analysis of 239 accessions. Third, usable density and distribution are important for genetic studies. The loci contained in the GBW16K array were selected with an average density of one target region per Mb and are uniformly distributed across the entire wheat genome, enabling a better cost performance without affecting the efficacy of the array in target application scenarios compared with the 15K, 35K, 50K, and 55K arrays.

### APR to stripe rust in Yaco“S”

Current evidence suggests that deployment of multiple effective resistance genes is a more effective method for increasing the longevity of resistance (Dracatos et al., 2023). For example, many wheat cultivars derived from CIMMYT (Huerta-Espino et al., 2020) and China (Liu et al., 2023a) have ongoing adequate to excellent resistance to stripe rust based on 2–8 resistance genes/QTLs (Supplemental Table 16) and continue

to maintain resistance. In this study, we found that the CIMMYT wheat line Yaco“S” contained resistance genes on chromosome arms 2BS, 2BL, and 3BS (Table 2). Based on location in the same chromosome interval, CDS sequence, and similar problems in seedling phenotyping across different genetic backgrounds, *QYr.nwafu-2BS* (*YrAc*) is *Yr27* (Athiyannan et al., 2022). *QYr.nwafu-3BS* likely includes *Yr30*, a backbone gene in the CIMMYT breeding program (Ellis et al., 2014) and pseudo-black chaff (PBC) associated with *Sr2* (Liu et al., 2022). *QYr.nwafu-2BL.4* was identified as a new major-effect APR locus effective in all test environments and mapped to a 2.0-cM interval between SNP markers *2B\_393939451* and *2B\_423802335* (Figure 5A and Table 2). Three main haplotypes in the *QYr.nwafu-2BL.4* interval were identified using the 660K array dataset for 1520 wheat accessions (Figure 5B). *Hap\_1*, present in Yaco“S”, was a favorable haplotype for stripe rust resistance; it was present in many CIMMYT and ICARDA cultivars and breeding lines but not in landraces and Chinese cultivars, indicating that *QYr.nwafu-2BL.4* has potential as a resource in Chinese breeding programs (Figure 5C and Supplemental Table 13).

Unlike ASR genes that usually encode typical NLR or receptor kinase proteins, APR genes appear to encode proteins with more variable protein structures (Dracatos et al., 2023). The three cloned APR genes, *Yr18*, *Yr36*, and *Yr46*, encode an ABC transporter (Krattinger et al., 2009), a kinase-START protein (Fu et al., 2009), and a hexose transporter (Moore et al., 2015), respectively. Through integrated micro-collinearity analysis, gene annotation, RNA-seq, and SNP data, we identified six potential high-confidence candidate genes in the *QYr.nwafu-2BL.4* interval (Figure 5D and 5E; Supplemental Figure 5; Supplemental Table 14). These six candidate genes were annotated differently from *Yr18*, *Yr36*, and *Yr46* (Figure 5E), implying that the cloning of *QYr.nwafu-2BL.4* will enrich knowledge of APR stripe rust

## Plant Communications

resistance proteins. Genes containing similar zinc-finger protein domains, *TraesCS2B01G300000* and *TraesCS2B01G297000* (Manser et al., 2024), and *TraesCS2B01G299700* with the TBC1 domain (Ge et al., 2022; Liu et al., 2023b), have been reported to participate in immunity, indicating that these three genes should be prioritized for functional verification experiments in future studies.

## METHODS

### Plant materials

An  $F_{5:6}$  Yaco“S” × MX169 (hereafter YM) RIL population containing 136 lines and a diversity panel of 239 wheat accessions (Supplemental Table 1) collected from different growing regions were used for validation of the GBW16K array. The RIL population was used in QTL mapping. Yaco“S” (HEIMA/COCORAQUE-75//NAC0ZARI-76; <http://wheatpedigree.net/>), developed by CIMMYT, has exhibited high levels of APR to stripe rust in the field from 2008 despite being susceptible at the seedling stage (Li et al., 2017). MX169 was susceptible at all growth stages and was also grown as a disease spreader. A secondary  $F_6$  population with 540 plants derived from RIL-YM106 was used in fine mapping of *QYr.nwafu-2BS* (*YrAc*). An  $F_6$ -resistant homozygote (YM106R) and an  $F_6$ -susceptible homozygote (YM106S) derived from RIL-YM106 were selected as an NIL pair. The Chinese cultivar Xiaoyan 22 was used as the susceptible control. A collection of 1520 wheat accessions previously phenotyped for stripe rust response and genotyped with the 660K SNP array was used for haplotype analysis (Liu et al., 2021). Ten wheat cultivars, namely Lantian19, Xinong865, Baomai6, Lantian27, Lantian15, Xinong979, Xingzi9104, Yangmai18, 92R137, and Lantian31, were used to evaluate the reproducibility of the GBW16k array.

### Selection and probe design for SNP regions

SNPs from the 660K SNP array dataset for 1520 wheat cultivars or lines (Liu et al., 2021) and whole-genome resequencing data for 20 bread wheat accessions from worldwide sources (Cheng et al., 2019) were used to design the GBTS chip. To retrieve high-quality SNP sites, SNPs with missing rate <60%, heterozygosity rate <20%, and MAF >0.01 were retained. Chromosome segments containing at least one SNP with a 120-bp window were reserved as candidate target-capture regions. Finally, totals of 342k and 840k candidate regions were obtained for a wheat GBTS liquid SNP array. Scores (GC content  $\geq 30\%$ , number of homologous sequences  $\leq 10$ ) were calculated for each candidate region. These scores, along with the MAF and polymorphic information content (PIC) values, were used to select candidate regions for which probes were designed. PIC was calculated by the method of Guo et al. (2019). The specificities of all probes from each marker region on the reference IWGSC RefSeq v.1.0 genome were assessed. The probe set was synthesized by a semiconductor-based *in situ* synthesis process.

### DNA extraction, library construction, and probe hybridization

Genomic DNA was extracted from fresh leaf samples using the cetyl trimethyl ammonium bromide method. DNA quality and concentration were evaluated by agarose gel electrophoresis and an Invitrogen Qubit 2.0 Fluorometer (Thermo Fisher Scientific, Carlsbad, CA, USA). DNA libraries were constructed by DNA fragmentation, end repair, adaptor ligation, and PCR. The quality of the enriched libraries was assessed using an Agilent 2100 Bioanalyzer (Agilent Technologies, Santa Clara, CA, USA) and an Invitrogen Qubit 2.0 Fluorometer. Equivalent double-stranded DNA libraries were pooled and transformed into a single-stranded circular DNA library by DNA denaturation and circularization. DNA nanoballs were generated from single-stranded circular DNA by rolling circle amplification, quantified using a Qubit ssDNA Assay kit (Thermo Fisher Scientific), and loaded onto the flow cell. Library hybridization capture was performed using the above probe set. A DNA library of 200- to 300-bp DNA fragments was constructed, after which 150-bp paired-end reads were sequenced

## GenoBaits WheatSNP16K array for genetic research

on a DNBSEQ-T7RS instrument (MGI, Shenzhen, China). All other experimental steps followed Guo et al. (2019) with the modifications described above.

### SNP and Indel calling, statistics, and annotation

Adaptors and low-quality reads were removed from raw reads using fastp (v.0.20.0, parameters: -n 10 -q 20 -u 40) (Chen et al., 2018). The resulting clean reads were aligned to the IWGSC RefSeq v.1.0 sequence using the Burrows-Wheeler aligner (Li and Durbin, 2009), followed by detection of SNP and Indel variants using the best-practice pipeline of the Genome Analysis Toolkit with the HaplotypeCaller function (Mckenna et al., 2010). Quality control for variations included criteria such as “MQ0  $\geq 4$  && ((MQ0/(1.0 \* DP)) > 0.1)” and “DP < 5 || QD < 2.” Variations with at least 5 $\times$  depth were considered valid for genotyping, and heterozygous genotypes were determined using an MAF of  $\geq 0.2$  and support from at least four reads for each allele. Marker density was calculated using a 500-kb window, and gap size was determined between adjacent markers on the same chromosome. Variations were annotated by ANOVA (Wang et al., 2010), considering a 3-kb up-/downstream distance. Only SNP sites, filtering samples with a missing rate >30%, followed by additional filtering for sites with a missing rate >50%, were retained. Finally, SNP sites with a minor allele number  $\geq 20$  and biallelic nature were retained for phylogenetic and population genetic analysis. A phylogenetic tree was generated using the NJ method implemented in “ape” in the R package (Alexander et al., 2009) and visualized with iTOL v.6 (Purcell et al., 2007).

### Linkage map construction

The filtering criteria of SNP markers for linkage map construction were as follows: PHR/polymorphic, <10% missing values, >5% MAF, and 1:1 segregation ratio confirmed by chi-squared tests ( $p > 0.001$ ). A linkage map was constructed using QTL IciMapping v.4.2 software and generated with Mapchart v.2.3 (Voorrips, 2002; Meng et al., 2015). Recombination fractions were converted to centimorgans (cM) using the Kosambi function (Kosambi 1943). One marker was selected from each co-segregating marker group using the “BIN” function. Selected markers were used to construct the genetic map using the “MAP” function.

### Phenotyping of stripe rust response

#### Field

Yaco“S,” MX169, and RILs were evaluated for adult-plant stage stripe rust reactions in four field environments: Yangling in Shaanxi province (34°17' N, 108°04' E) in 2020 (20YL) and 2021 (21YL) and Jiangyou in Sichuan province (31°76' N, 104°72' E) in 2021 (21JY) and Tianshui in Gansu province (34°89' N, 106°01' E) in 2021 (21TS). YM106  $F_6$  and YM106  $F_{6:7}$  populations were tested for stripe rust reaction at Yangling in 2021 (21YL) and 2022 (22YL), respectively. Jiangyou and Tianshui are locations with regular natural occurrence of stripe rust. All MX169 rows in Yangling were inoculated with a urediniospore mixture of prevalent *Pst* races (CYR32, CYR33, and CYR34) suspended in liquid paraffin (1:300) during late March each year. The avirulence/virulence profiles of the races are given in Wu et al. (2016). A randomized complete block design with two replications was used in all environments. Each plot was a 1-m row with 25-cm row spacing, and 15–20 seeds were planted in each plot. Two rows of the highly susceptible cultivar Xiaoyan22 were planted after every 20 rows, and MX169 was planted adjacent to the plot area to ensure uniform disease development. IT based on a 0–9 scale (Line and Qayoum, 1992) and DS based on the modified Cobb scale (Peterson et al., 1948) were recorded for each line beginning when the DS on the susceptible controls Xiaoyan22 and MX169 was about 60%, then recorded weekly until the disease reached maximum levels.

#### Greenhouse

The NILs YM106R and YM106S were grown in the greenhouse to assess the resistance conferred by *YrAc*, with MX169 as the susceptible control. Ten to fifteen plants of each line growing in 20 × 20 × 15-cm plastic pots were inoculated with *Pst* race CYR34 at the two-, three-, four-, and five-leaf stages. After inoculation, plants were kept in a dark dew chamber

at 10°C for 24 h, then transferred to a greenhouse with a daily cycle of light (20 000 lux) at 16°C ± 2°C for 14 h and darkness at 10°C ± 2°C for 10 h. ITs were recorded for YM106R and YM106S at 15–18 days post inoculation. The tests were repeated three times to ensure phenotypic reliability.

### Statistical analysis of phenotypic data

Both IT and DS data from all environments were statistically analyzed. Frequency distributions of population phenotypic data were generated, and *t*-tests were performed in Excel 2019. Phenotypic variation, broad-sense heritability ( $H^2$ ), and Pearson's correlations between environments were calculated on the basis of the mean IT and DS using the "AOV" function in QTL IciMapping v.4.2 with default parameters (Meng et al., 2015).  $H^2$  was estimated according to Allard (1960) using the equation  $h^2 b = \sigma^2 g / (\sigma^2 g + \sigma^2 ge/e + \sigma^2 \varepsilon/re)$ , with  $\sigma^2 g$ ,  $\sigma^2 ge$ , and  $\sigma^2 r$  representing genotype (line), genotype × environment, and error variances, respectively. *e* and *r* represent the numbers of environments and replicates.

### KASP marker development

KASP markers based on a subset of polymorphic SNPs from the GBW16K or 660K SNP genotype arrays for Yaco"S" and MX169 were developed to narrow down intervals for MAS of target resistance loci (Supplemental Table 10). Linkage of QTLs and polymorphism of KASP markers were assessed on the RIL population. Primers were designed on the Polymarker platform (<http://www.polymarker.info/>) using sequences flanking the SNPs. The PCR composition and procedure were described previously (Liu et al., 2021).

### QTL analysis

Inclusive composite interval mapping with the additive tool (ICIM-ADD) in IciMapping v.4.2 (Meng et al., 2015) was performed to detect QTLs based on IT and DS scores from each environment. Likelihood-of-odds (LOD) thresholds for declaring statistical significance were calculated by 1000 permutations at a *p* value ≤ 0.01. The LOD significance threshold estimated for each trait was 3.8. The phenotypic variances explained by individual QTLs and additive effects at the LOD peaks were also obtained. Physical positions in IWGSC RefSeq v.1.0 were obtained by blast using the flanking marker sequences for each QTL (<http://wheatomics.sdau.edu.cn/>) (Ma et al., 2021). QTLs were named according to the international rules of genetic nomenclature (Boden et al., 2023). The abbreviations "Yr" and "nwafu" were used for "stripe rust resistance" and "Northwest A&F University," respectively. Fine mapping of *QYr.nwafu-2BS* was also performed in this study. All 560 YM106\_F6 plants were genotyped with KASP markers on chromosome arm 2BS, and recombination events were identified. A high-resolution genetic map was constructed using JoinMap v.4.0 (<https://www.kyazma.nl>) and visualized with Mapchart v.2.0 (Voorrips, 2002).

### Comparisons with reported stripe rust resistance genes/QTLs

To determine the novelty of loci identified in this study, we compared the relative physical distances identified here with previously reported Yr genes/QTLs on the basis of location in IWGSC RefSeq v.1.0. The sequences of the closest flanking markers identified in genetic populations and significant markers detected in GWAS were blasted against IWGSC RefSeq v.1.0 on WheatOmics 1.0 (<http://wheatomics.sdau.edu.cn/>) to obtain confidence intervals for each previously reported stripe rust resistance gene/QTL (Ma et al., 2021).

### RNA-seq

Fresh leaves of Yaco"S" and MX169 inoculated with a urediniospore mixture of *Pst* races (CYR32, CYR33, and CYR34) were sampled at 0, 1, and 2 days post inoculation. Two sample bulks were prepared by mixing equal amounts of leaf tissue from each time point, and the total RNA was extracted. RNA quality and concentration were determined using a NanoDrop instrument and a fragment analyzer. Each sample was prepared to construct a 350-bp paired-end library with the Bioruptor Pico Sonication

System (Diagenode) and sequenced on the DNBseq-20000 platform at Beijing Genomics Institute (BGI, Beijing; <https://www.bgi.com/>) to obtain 12 Gbp of total data/40 M reads per sample. Low-quality bases and adapter sequences in the raw reads were filtered out to obtain clean reads and high-quality data. The clean reads were aligned to the reference genome sequence to identify unique reads and anchor the physical position on IWGSC RefSeq v.2.1 (Zhu et al., 2021) with HISAT2 v.2.1.0 (Kim et al., 2015) and quantified using StringTie v.1.3.5 (Pertea et al., 2016).

### Haplotype analysis in the *QYr.nwafu-2BL.4* interval

660K SNP array data in the target interval of *QYr.nwafu-2BL.4* for 1520 wheat accessions were used for haplotype analysis. A phylogenetic analysis was performed using MEGA 7.0.26, and the NJ tree was visualized with the online tool iTOL (<https://itol.embl.de/>) (Letunic and Bork, 2024). Accessions grouped in the same branch were considered to be the same haplotype. Haplotypes with the lowest IT and DS were considered superior.

### Candidate gene analysis

Annotated genes within the precisely mapped interval on IWGSC RefSeq v.1.0 and v.2.1 were queried using WheatOmics 1.0 (<http://wheatomics.sdau.edu.cn/>) (Ma et al., 2021). Candidate genes were confirmed on the basis of three criteria: including functional annotation as disease resistance related, expression in resistant parent Yaco"S," and synonymous sequence variation between the CDSs of Yaco"S" and MX169.

The cDNA sequences for the candidate gene *TraesCS2B01G182800* in Yaco"S" and MX169 were confirmed by PCR amplification using gene-specific primers according to Si et al. (2021). The reaction mixture for PCR contained 200 ng cDNA, 12.5 μL Prime STAR Mix (New England Biolabs, Beverly, MA, USA), 10 μM forward primer, 10 μM reverse primer, and ddH<sub>2</sub>O added to obtain 25 μL. PCR was initiated with a 2-min denaturation step at 98°C, followed by 35 cycles at 98°C for 10 s, 56°C for 15 s, and 72°C for 90 s, completion at 72°C for 5 min, and transfer to 6°C. Sanger sequencing was performed by Beijing Tsingke Biotech. Sequence alignment for the CDSs of *TraesCS2B01G182800* in Yaco"S" and MX169 with Yr27 was performed in DNAMAN (<https://www.lynnon.com/dnaman.html>) to confirm whether YrAc and Yr27 were the same gene, and the results were visualized using SnapGene Viewer ([www.snapgene.com](http://www.snapgene.com)).

### DATA AND CODE AVAILABILITY

Raw sequence reads are deposited in the National Genomics Data Center (BioProject PRJCA030369). The mSNP genotype data for 239 wheat lines and the coding sequence of *TraesCS2B01G182800* were deposited at figshare (<https://figshare.com/projects/GBW16K/221464>). All data, models, and code generated or used during the study are available from the corresponding author on request.

### FUNDING

This study was financially supported by the National Key R&D Program of China (2021YFD1200600), International Cooperation and Exchange of the National Natural Science Foundation of China (grant no. 31961143019), the National Science Foundation for Young Scientists in China (grant no. 32302377), the National Natural Science Foundation of China (grant nos. 32272088 and 32372562), and the Major Program of the National Natural Science Foundation of China (32293240).

### ACKNOWLEDGMENTS

We are grateful to Prof. R.A. McIntosh, Plant Breeding Institute, University of Sydney, for language editing and proofreading of the draft manuscript; Dr. Xuelling Huang for KASP genotyping; Ms. Haiying Wang for construction of cDNA library; and the HPC of NWFU for technical server support. The Northwest A&F University has filed a patent application (number ZL 2022 1 0046225.5) on the use of the probes of the GenoBaits

## Plant Communications

WheatSNP16K array, in which Q.Z., S.L., M.X., J.W., W.Z., C.L., F.Y., Z.K., and D.H. are listed as inventors.

### AUTHOR CONTRIBUTIONS

S.L., Q.Z., D.H., and Z.K. conceived and designed the experiments and composed the manuscript. S.L., Q.Z., M.X., X.W., J.W., J.L., X.C., H.L., F.Y., and S.H. performed the experiments. S.L., Q.Z., M.X., and X.W. analyzed the data. R.P.S., S.B., C.L., and W.Z. provided expertise and feedback.

### SUPPLEMENTAL INFORMATION

Supplemental information is available at *Plant Communications Online*.

Received: March 4, 2024

Revised: August 5, 2024

Accepted: September 23, 2024

Published: September 24, 2024

### REFERENCES

- Alexander, D.H., Novembre, J., and Lange, K.** (2009). Fast model-based estimation of ancestry in unrelated individuals. *Genome Res.* **19**:1655–1664.
- Allard, R.W.** (1960). *Principles of Plant Breeding* (John Wiley and Sons Inc).
- Allen, A.M., Winfield, M.O., Burrige, A.J., Downie, R.C., Benbow, H.R., Barker, G.L.A., Wilkinson, P.A., Coghill, J., Waterfall, C., Davassi, A., et al.** (2017). Characterization of a wheat breeders array suitable for high-throughput SNP genotyping of global accessions of hexaploid bread wheat (*Triticum aestivum*). *Plant Biotechnol. J.* **15**:390–401.
- Athiyannan, N., Abrouk, M., Boshoff, W.H.P., Cauet, S., Rodde, N., Kudrna, D., Mohammed, N., Bettgenhaeuser, J., Botha, K.S., Derman, S.S., et al.** (2022). Long-read genome sequencing of bread wheat facilitates disease resistance gene cloning. *Nat. Genet.* **54**:227–231.
- Boden, S.A., McIntosh, R.A., Uauy, C., Krattinger, S.G., Dubcovsky, J., Rogers, W.J., Xia, X.C., Badaeva, E.D., Bentley, A.R., Brown-Guedira, G., et al.** (2023). Updated guidelines for gene nomenclature in wheat. *Theor. Appl. Genet.* **136**:72.
- Boukhatem, N., Baret, P.V., Mingeot, D., Jacquemin, J.M., and Du, Y.** (2002). Quantitative trait loci for resistance against yellow rust in two wheat-derived recombinant inbred line populations. *Theor. Appl. Genet.* **104**:111–118.
- Buerstmayr, M., Matiasch, L., Mascher, F., Vida, G., Ittu, M., Robert, O., Holdgate, S., Flath, K., Neumayer, A., and Buerstmayr, H.** (2014). Mapping of quantitative adult plant field resistance to leaf rust and stripe rust in two European winter wheat populations reveals co-location of three QTL conferring resistance to both rust pathogens. *Theor. Appl. Genet.* **127**:2011–2028.
- Chen, S., Zhou, Y., Chen, Y., and Gu, J.** (2018). Fastp: an ultra-fast all-in-one FASTQ preprocessor. *Bioinformatics* **34**:i884–i890.
- Chen, X.M., and Kang, Z.S.** (2017). Chapter 5 - Stripe rust resistance. In *Stripe Rust*, X.M. Chen and Z.S. Kang, eds. (Springer), pp. 353–558.
- Cheng, B., Gao, X., Cao, N., Ding, Y., Chen, T., Zhou, Q., Gao, Y., Xin, Z., and Zhang, L.** (2022). QTL mapping for adult plant resistance to wheat stripe rust in a M96-5 × Guixie 3 wheat population. *J. Appl. Genet.* **63**:265–279.
- Cheng, H., Liu, J., Wen, J., Nie, X., Xu, L., Chen, N., Li, Z., Wang, Q., Zheng, Z., Li, M., et al.** (2019). Frequent intra- and inter-species introgression shapes the landscape of genetic variation in bread wheat. *Genome Biol.* **20**:136.
- GenoBaits WheatSNP16K array for genetic research**
- Cheng, P., and Chen, X.M.** (2010). Molecular mapping of a gene for stripe rust resistance in spring wheat cultivar IDO377s. *Theor. Appl. Genet.* **121**:195–204.
- Chhetri, M., Miah, H., Wong, D., Hayden, M., Bansal, U., and Bariana, H.** (2023). Mapping of a stripe rust resistance gene *Yr72* in the common wheat landraces AUS27506 and AUS27894 from the Watkins collection. *Genes* **14**:1993.
- Christiansen, M.J., Feenstra, B., Skovgaard, I.M., and Andersen, S.B.** (2006). Genetic analysis of resistance to yellow rust in hexaploid wheat using a mixture model for multiple crosses. *Theor. Appl. Genet.* **112**:581–591.
- Cobo, N., Wanjugi, H., Lagudah, E., and Dubcovsky, J.** (2019). A high-resolution map of wheat *Qyr.ucw-1BL*, an adult plant stripe rust resistance locus in the same chromosomal region as *Yr29*. *Plant Genome* **12**:180055.
- Dracatos, P.M., Lu, J., Sánchez Martín, J., and Wulff, B.B.H.** (2023). Resistance that stacks up: engineering rust and mildew disease control in the cereal crops wheat and barley. *Plant Biotechnol. J.* **21**:1938–1951.
- Draz, I.S., Serfling, A., Muqaddasi, Q.H., and Röder, M.S.** (2021). Quantitative trait loci for yellow rust resistance in spring wheat doubled haploid populations developed from the German federal ex situ genebank genetic resources. *Plant Genome* **14**:e20142.
- Ellis, J.G., Lagudah, E.S., Spielmeier, W., and Dodds, P.N.** (2014). The past, present and future of breeding rust resistant wheat. *Front. Plant Sci.* **5**:641.
- Farzand, M., Dhariwal, R., Hiebert, C.W., Spaner, D., and Randhawa, H.S.** (2021). Mapping quantitative trait loci associated with stripe rust resistance from the Canadian wheat cultivar ‘AAC Innova. *Can J Plant Pathol* **43**:S227–S241.
- Fu, D., Uauy, C., Distelfeld, A., Blechl, A., Epstein, L., Chen, X., Sela, H., Fahima, T., and Dubcovsky, J.** (2009). A novel kinase-START gene confers temperature-dependent resistance to wheat stripe rust. *Science* **323**:1357–1360.
- Ge, P., Lei, Z., Yu, Y., Lu, Z., Qiang, L., Chai, Q., Zhang, Y., Zhao, D., Li, B., Pang, Y., et al.** (2022). *M. tuberculosis* PknG manipulates host autophagy flux to promote pathogen intracellular survival. *Autophagy* **18**:576–594.
- Grassini, P., Eskridge, K.M., and Cassman, K.G.** (2013). Distinguishing between yield advances and yield plateaus in historical crop production trends. *Nat. Commun.* **4**:2918.
- Guo, Q., Zhang, Z.J., Xu, Y.B., Li, G.H., Feng, J., and Zhou, Y.** (2008). Quantitative trait loci for high-temperature adult-plant and slow-rusting resistance to *Puccinia striiformis* f. sp. *tritici* in wheat cultivars. *Phytopathology* **98**:803–809.
- Guo, Z., Wang, H., Tao, J., Ren, Y., Xu, C., Wu, K., Zou, C., Zhang, J., and Xu, Y.** (2019). Development of multiple SNP marker panels affordable to breeders through genotyping by target sequencing (GBTS) in maize. *Mol. Breed.* **39**:37.
- Guo, Z., Yang, Q., Huang, F., Zheng, H., Sang, Z., Xu, Y., Zhang, C., Wu, K., Tao, J., Prasanna, B.M., et al.** (2021). Development of high-resolution multiple-SNP arrays for genetic analyses and molecular breeding through genotyping by target sequencing and liquid chip. *Plant Commun.* **2**:100230.
- Haudry, A., Cenci, A., Ravel, C., Bataillon, T., Brunel, D., Poncet, C., Hochu, I., Poirier, S., Santoni, S., Glémin, S., and David, J.** (2007). Grinding up wheat: a massive loss of nucleotide diversity since domestication. *Mol. Biol. Evol.* **24**:1506–1517.
- He, F., Pasam, R., Shi, F., Kant, S., Keeble-Gagnere, G., Kay, P., Forrest, K., Fritz, A., Hucl, P., Wiebe, K., et al.** (2019). Exome sequencing highlights the role of wild-relative introgression in

- shaping the adaptive landscape of the wheat genome. *Nat. Genet.* **51**:896–904.
- Hewitt, T., Zhang, J., Huang, L., Upadhyaya, N., Li, J., Park, R., Hoxha, S., McIntosh, R., Lagudah, E., and Zhang, P. (2021). Wheat leaf rust resistance gene *Lr13* is a specific *Ne2* allele for hybrid necrosis. *Mol. Plant* **14**:1025–1028.
- Hou, L., Chen, X., Wang, M., See, D.R., Chao, S., Bulli, P., and Jing, J. (2015). Mapping a large number of QTL for durable resistance to stripe rust in winter wheat Druchamp using SSR and SNP markers. *PLoS One* **10**:e0126794.
- Huang, S., Zhang, Y., Ren, H., Zhang, X., Yu, R., Liu, S., Zeng, Q., Wang, Q., Yuan, F., Singh, R.P., et al. (2023). High density mapping of wheat stripe rust resistance gene *QYrxn3517-1BL* using QTL mapping, BSE-seq and candidate gene analysis. *Theor. Appl. Genet.* **136**:39.
- Huerta-Espino, J., Singh, R., Crespo-Herrera, L.A., Villaseñor-Mir, H.E., Rodriguez-Garcia, M.F., Dreisigacker, S., Barcenas-Santana, D., and Lagudah, E. (2020). Adult plant slow rusting genes confer high levels of resistance to rusts in bread wheat cultivars from Mexico. *Front. Plant Sci.* **11**:824.
- International Wheat Genome Sequencing Consortium (IWGSC). (2018). Shifting the limits in wheat research and breeding using a fully annotated reference genome. *Science* **361**:eaar7191.
- Jayakodi, M., Padmarasu, S., Haberer, G., Bonthala, V.S., Gundlach, H., Monat, C., Lux, T., Kamal, N., Lang, D., Himmelbach, A., et al. (2020). The barley pan-genome reveals the hidden legacy of mutation breeding. *Nature* **588**:284–289.
- Jighly, A., Oyiga, B.C., Makdis, F., Nazari, K., Youssef, O., Tadesse, W., Abdalla, O., and Ogbonnaya, F.C. (2015). Genome-wide DArT and SNP scan for QTL associated with resistance to stripe rust (*Puccinia striiformis* f. sp. *tritici*) in elite ICARDA wheat (*Triticum aestivum* L.) Germplasm. *Theor. Appl. Genet.* **128**:1277–1295.
- Juliana, P., Poland, J., Huerta-Espino, J., Shrestha, S., Crossa, J., Crespo-Herrera, L., Toledo, F.H., Govindan, V., Mondal, S., Kumar, U., et al. (2019). Improving grain yield, stress resilience and quality of bread wheat using large-scale genomics. *Nat. Genet.* **51**:1530–1539.
- Kale, S.M., Schulthess, A.W., Padmarasu, S., Boeven, P.H.G., Schacht, J., Himmelbach, A., Steuernagel, B., Wulff, B.B.H., Reif, J.C., Stein, N., and Mascher, M. (2022). A catalogue of resistance gene homologs and a chromosome-scale reference sequence support resistance gene mapping in winter wheat. *Plant Biotechnol. J.* **20**:1730–1742.
- Kim, D., Langmead, B., and Salzberg, S.L. (2015). HISAT: a fast spliced aligner with low memory requirements. *Nat. Methods* **12**:357–360.
- Kosambi, D.D. (1943). The estimation of map distances from recombination values. *Ann. Eugen.* **12**:172–175.
- Krattinger, S.G., Lagudah, E.S., Spielmeier, W., Singh, R.P., Huerta-Espino, J., McFadden, H., Bossolini, E., Selter, L.L., and Keller, B. (2009). A putative ABC transporter confers durable resistance to multiple fungal pathogens in wheat. *Science* **323**:1360–1363.
- Kumar, A., Chhuneja, P., Jain, S., Kaur, S., Balyan, H.S., and Gupta, P. (2013). Mapping main effect QTL and epistatic interactions for leaf rust and yellow rust using high density ITMI linkage map. *Aust. J. Crop. Sci.* **7**:492–499.
- Lagudah, E.S., Krattinger, S.G., Herrera-Foessel, S., Singh, R.P., Huerta-Espino, J., Spielmeier, W., Brown-Guedira, G., Selter, L.L., and Keller, B. (2009). Gene-specific markers for the wheat gene *Lr34/Yr18/Pm38* which confers resistance to multiple fungal pathogens. *Theor. Appl. Genet.* **119**:889–898.
- Li, H., Wang, Q., Xu, L., Mu, J., Wu, J., Zeng, Q., Yu, S., Huang, L., Han, D., and Kang, Z. (2017). Rapid identification of a major effect QTL conferring adult plant resistance to stripe rust in wheat cultivar Yaco “S”. *Euphytica* **213**:124.
- Letunic, I., and Bork, P. (2024). Interactive Tree of Life (iTOL) v6: recent updates to the phylogenetic tree display and annotation tool. *Nucleic. Acids Res.* **52**:W78–W82.
- Li, H., and Durbin, R. (2009). Fast and accurate short read alignment with burrows-wheeler transform. *Bioinformatics* **25**:1754–1760.
- Line, R.F., and Qayoum, A. (1992). Virulence, aggressiveness, evolution and distribution of races of *Puccinia striiformis* (the cause of stripe rust of wheat) in North America, 1968–1987.
- Liu, J., He, Z., Wu, L., Bai, B., Wen, W., Xie, C., and Xia, X. (2015). Genome-wide linkage mapping of QTL for adult-plant resistance to stripe rust in a Chinese wheat population Linmai 2 x Zhong 892. *PLoS One* **10**:e145462.
- Liu, S., Huang, S., Zeng, Q., Wang, X., Yu, R., Wang, Q., Singh, R.P., Bhavani, S., Kang, Z., Wu, J., and Han, D. (2021). Refined mapping of stripe rust resistance gene *YrP10090* within a desirable haplotype for wheat improvement on chromosome 6A. *Theor. Appl. Genet.* **134**:2005–2021.
- Liu, S., Liu, D., Zhang, C., Zhang, W., Wang, X., Mi, Z., Gao, X., Ren, Y., Lan, C., Liu, X., et al. (2023a). Slow stripe rusting in Chinese wheat Jimai 44 conferred by *Yr29* in combination with a major QTL on chromosome arm 6AL. *Theor. Appl. Genet.* **136**:175.
- Liu, S., Wang, X., Zhang, Y., Jin, Y., Xia, Z., Xiang, M., Huang, S., Qiao, L., Zheng, W., Zeng, Q., et al. (2022). Enhanced stripe rust resistance obtained by combining *Yr30* with a widely dispersed, consistent QTL on chromosome arm 4BL. *Theor. Appl. Genet.* **135**:351–365.
- Liu, Y., Liu, S., Zhang, Z., Ni, L., Chen, X., Ge, Y., Zhou, G., and Tian, Z. (2022c). GenoBaits Soy40K: a highly flexible and low-cost SNP array for soybean studies. *Sci. China Life Sci.* **65**:1898–1901.
- Liu, Z., Shang, F., Li, N., and Dong, W. (2023b). TBC1 domain family member 25 protects against myocardial apoptosis and the proinflammatory response triggered by is chemia-reperfusion injury through suppression of the TAK1-JNK/p38 MAPK signaling cascade. *In Vitro Cell. Dev. Biol. Anim.* **59**:796–810.
- Ma, S., Wang, M., Wu, J., Guo, W., Chen, Y., Li, G., Wang, Y., Shi, W., Xia, G., Fu, D., et al. (2021). WheatOmics: A platform combining multiple omics data to accelerate functional genomics studies in wheat. *Mol. Plant* **14**:1965–1968.
- Mago, R., Simkova, H., Brown-Guedira, G., Dreisigacker, S., Breen, J., Jin, Y., Singh, R., Appels, R., Lagudah, E.S., Ellis, J., et al. (2011a). An accurate DNA marker assay for stem rust resistance gene *Sr2* in wheat. *Theor. Appl. Genet.* **122**:735–744.
- Mago, R., Tabe, L., McIntosh, R.A., Pretorius, Z., Kota, R., Paux, E., Wicker, T., Breen, J., Lagudah, E.S., Ellis, J.G., and Spielmeier, W. (2011b). A multiple resistance locus on chromosome arm 3BS in wheat confers resistance to stem rust (*Sr2*), leaf rust (*Lr27*) and powdery mildew. *Theor. Appl. Genet.* **123**:615–623.
- Mallard, S., Gaudet, D., Aldeia, A., Abelard, C., Besnard, A.L., Sourdil, P., and Dedryver, F. (2005). Genetic analysis of durable resistance to yellow rust in bread wheat. *Theor. Appl. Genet.* **110**:1401–1409.
- Manser, B., Zbinden, H., Herren, G., Steger, J., Isaksson, J., Bräunlich, S., Wicker, T., and Keller, B. (2024). Wheat zinc finger protein TaZF interacts with both the powdery mildew *AvrPm2* protein and the corresponding wheat *Pm2a* immune receptor. *Plant Commun.* **5**:100769.
- Marchal, C., Zhang, J., Zhang, P., Fenwick, P., Steuernagel, B., Adamski, N.M., Boyd, L., McIntosh, R., Wulff, B.B.H., Berry, S., et al. (2018). BED-domain-containing immune receptors confer diverse resistance spectra to yellow rust. *Nat. Plants* **4**:662–668.

## Plant Communications

- McKenna, A., Hanna, M., Banks, E., Sivachenko, A., Cibulskis, K., Kernytsky, A., Garimella, K., Altshuler, D., Gabriel, S., Daly, M., and DePristo, M.A. (2010). The genome analysis Toolkit: a MapReduce framework for analyzing next-generation DNA sequencing data. *Genome Res.* **20**:1297–1303.
- Meng, L., Li, H., Zhang, L., and Wang, J. (2015). QTL IciMapping: Integrated software for genetic linkage map construction and quantitative trait locus mapping in biparental populations. *Crop J.* **3**:269–283.
- Moore, J.W., Herrera-Foessel, S., Lan, C., Schnippenkoetter, W., Ayliffe, M., Huerta-Espino, J., Lillemo, M., Viccars, L., Milne, R., Periyannan, S., et al. (2015). A recently evolved hexose transporter variant confers resistance to multiple pathogens in wheat. *Nat. Genet.* **47**:1494–1498.
- Niu, J., Ma, S., Zheng, S., Zhang, C., Lu, Y., Si, Y., Tian, S., Shi, X., Liu, X., Naeem, M.K., et al. (2023). Whole-genome sequencing of diverse wheat accessions uncovers genetic changes during modern breeding in China and the United States. *Plant Cell* **35**:4199–4216.
- Pailard, S., Trotoux-Verplancke, G., Perretant, M.R., Mohamadi, F., Leconte, M., Coëdel, S., de Vallavieille-Pope, C., and Dedyver, F. (2012). Durable resistance to stripe rust is due to three specific resistance genes in French bread wheat cultivar Apache. *Theor. Appl. Genet.* **125**:955–965.
- Pertea, M., Kim, D., Pertea, G.M., Leek, J.T., and Salzberg, S.L. (2016). Transcript-level expression analysis of RNA-seq experiments with HISAT, StringTie and Ballgown. *Nat. Protoc.* **11**:1650–1667.
- Peterson, R.F., Campbell, A.B., and Hannah, A.E. (1948). A diagrammatic scale for estimating rust intensity on leaves and stems of cereals. *Can. J. Res.* **26c**:496–500.
- Pont, C., Leroy, T., Seidel, M., Tondelli, A., Duchemin, W., Armisen, D., Lang, D., Bustos-Korts, D., Goué, N., Balfourier, F., et al. (2019). Tracing the ancestry of modern bread wheats. *Nat. Genet.* **51**:905–911.
- Powell, N.M., Lewis, C.M., Berry, S.T., MacCormack, R., and Boyd, L.A. (2013). Stripe rust resistance genes in the UK winter wheat cultivar Claire. *Theor. Appl. Genet.* **126**:1599–1612.
- Purcell, S., Neale, B., Todd-Brown, K., Thomas, L., Ferreira, M.A.R., Bender, D., Maller, J., Sklar, P., de Bakker, P.I.W., Daly, M.J., and Sham, P.C. (2007). PLINK: a tool set for whole-genome association and population-based linkage analyses. *Am. J. Hum. Genet.* **81**:559–575.
- Qiao, L., Li, H., Wang, J., Zhao, J., Zheng, X., Wu, B., Du, W., Wang, J., and Zheng, J. (2021). Analysis of genetic regions related to field grain number per spike from Chinese wheat founder parent Linfen 5064. *Front. Plant Sci.* **12**:808136.
- Ramburan, V.P., Pretorius, Z.A., Louw, J.H., Boyd, L.A., Smith, P.H., Boshoff, W.H.P., and Prins, R. (2004). A genetic analysis of adult plant resistance to stripe rust in the wheat cultivar Kariega. *Theor. Appl. Genet.* **108**:1426–1433.
- Ren, Y., He, Z., Li, J., Lillemo, M., Wu, L., Bai, B., Lu, Q., Zhu, H., Zhou, G., Du, J., et al. (2012). QTL mapping of adult-plant resistance to stripe rust in a population derived from common wheat cultivars Naxos and Shanghai 3/Catbird. *Theor. Appl. Genet.* **125**:1211–1221.
- Ren, Y., Liu, L.S., He, Z.H., Wu, L., Bai, B., and Xia, X.C. (2015). QTL mapping of adult-plant resistance to stripe rust in a “Lumai 21 × Jingshuang 16” wheat population. *Plant Breed.* **134**:501–507.
- Rosewarne, G.M., Singh, R.P., Huerta-Espino, J., and Rebetzke, G.J. (2008). Quantitative trait loci for slow-rusting resistance in wheat to leaf rust and stripe rust identified with multi-environment analysis. *Theor. Appl. Genet.* **116**:1027–1034.
- Schulthess, A.W., Kale, S.M., Liu, F., Zhao, Y., Philipp, N., Rembe, M., Jiang, Y., Beukert, U., Serfling, A., Himmelbach, A., et al. (2022). **GenoBaits WheatSNP16K array for genetic research**
- Genomics-informed prebreeding unlocks the diversity in genebanks for wheat improvement. *Nat. Genet.* **54**:1544–1552.
- Si, Y., Zheng, S., Niu, J., Tian, S., Gu, M., Lu, Q., He, Y., Zhang, J., Shi, X., Li, Y., and Ling, H.Q. (2021). *Ne2*, a typical CC-NBS-LRR-type gene, is responsible for hybrid necrosis in wheat. *New Phytol.* **232**:279–289.
- Singh, A., Pandey, M.P., Singh, A.K., Knox, R.E., Ammar, K., Clarke, J.M., Clarke, F.R., Singh, R.P., Pozniak, C.J., DePauw, R.M., et al. (2013). Identification and mapping of leaf, stem and stripe rust resistance quantitative trait loci and their interactions in durum wheat. *Mol. Breed.* **31**:405–418.
- Singh, K., Saini, D.K., Saripalli, G., Batra, R., Gautam, T., Singh, R., Pal, S., Kumar, M., Jan, I., Singh, S., et al. (2022). WheatQTLdb v2.0: a supplement to the database for wheat QTL. *Mol. Breed.* **42**:56.
- Sui, X.X., Wang, M.N., and Chen, X.M. (2009). Molecular mapping of a stripe rust resistance gene in spring wheat cultivar Zak. *Phytopathology* **99**:1209–1215.
- Sun, C., Dong, Z., Zhao, L., Ren, Y., Zhang, N., and Chen, F. (2020). The wheat 660k SNP array demonstrates great potential for marker-assisted selection in polyploid wheat. *Plant Biotechnol. J.* **18**:1354–1360.
- Sun, Z., Zheng, Z., Qi, F., Wang, J., Wang, M., Zhao, R., Liu, H., Xu, J., Qin, L., Dong, W., et al. (2023). Development and evaluation of the utility of GenoBaits peanut 40k for a peanut MAGIC population. *Mol. Breed.* **43**:72.
- Tewhey, R., Warner, J.B., Nakano, M., Libby, B., Medkova, M., David, P.H., Kotsopoulos, S.K., Samuels, M.L., Hutchison, J.B., Larson, J.W., et al. (2009). Microdroplet-based PCR enrichment for large-scale targeted sequencing. *Nat. Biotechnol.* **27**:1025–1031.
- Tian, Z., Wang, J.W., Li, J., and Han, B. (2021). Designing future crops: challenges and strategies for sustainable agriculture. *Plant J.* **105**:1165–1178.
- van Dijk, M., Morley, T., Rau, M.L., and Saghai, Y. (2021). A meta-analysis of projected global food demand and population at risk of hunger for the period 2010–2050. *Nat. Food* **2**:494–501.
- Vazquez, M.D., Zemetra, R., Peterson, C.J., Chen, X.M., Heesacker, A., and Mundt, C.C. (2015). Multi-location wheat stripe rust QTL analysis: genetic background and epistatic interactions. *Theor. Appl. Genet.* **128**:1307–1318.
- Voorrips, R.E. (2002). Mapchart: software for the graphical presentation of linkage maps and QTLs. *J. Hered.* **93**:77–78.
- Walkowiak, S., Gao, L., Monat, C., Haberer, G., Kassa, M.T., Brinton, J., Ramirez-Gonzalez, R.H., Kolodziej, M.C., Delorean, E., Thambugala, D., et al. (2020). Multiple wheat genomes reveal global variation in modern breeding. *Nature* **588**:277–283.
- Wang, J., Yang, C., Zhao, W., Wang, Y., Qiao, L., Wu, B., Zhao, J., Zheng, X., Wang, J., and Zheng, J. (2022). Genome-wide association study of grain hardness and novel Puroindoline alleles in common wheat. *Mol. Breed.* **42**:40.
- Wang, K., Li, M., and Hakonarson, H. (2010). ANNOVAR: functional annotation of genetic variants from high-throughput sequencing data. *Nucleic Acids Res.* **38**:e164.
- Wellings, C.R. (2011). Global status of stripe rust: a review of historical and current threats. *Euphytica* **179**:129–141.
- Wu, J., Wang, Q., Chen, X., Wang, M., Mu, J., Lv, X., Huang, L., Han, D., and Kang, Z. (2016). Stripe rust resistance in wheat breeding lines developed for central Shaanxi, an overwintering region for *Puccinia striiformis* f. sp. *tritici* in China. *Can J Plant Pathol* **38**:317–324.
- Wu, J., Yu, R., Wang, H., Zhou, C., Huang, S., Jiao, H., Yu, S., Nie, X., Wang, Q., Liu, S., et al. (2021). A large-scale genomic association analysis identifies the candidate causal genes conferring stripe rust

- resistance under multiple field environments. *Plant Biotechnol. J.* **19**:177–191.
- Xu, L.S., Wang, M.N., Cheng, P., Kang, Z.S., Hulbert, S.H., and Chen, X.M.** (2013). Molecular mapping of *Yr53*, a new gene for stripe rust resistance in durum wheat accession PI 480148 and its transfer to common wheat. *Theor. Appl. Genet.* **126**:523–533.
- Xu, Y., Yang, Q., Zheng, H., Xu, Y., Sang, Z., Guo, Z., Peng, H., Zhang, C., Lan, H., Wang, Y., et al.** (2020). Genotyping by target sequencing (GBTS) and its applications. *Sci. Agric. Sin.* **53**:2983–3004.
- Yan, X., Li, M., Zhang, P., Yin, G., Zhang, H., Gebrewahid, T.W., Zhang, J., Dong, L., Liu, D., Liu, Z., and Li, Z.** (2021). High-temperature wheat leaf rust resistance gene *Lr13* exhibits pleiotropic effects on hybrid necrosis. *Mol. Plant* **14**:1029–1032.
- Zegeye, H., Rasheed, A., Makdis, F., Badebo, A., and Ogonnaya, F.C.** (2014). Genome-wide association mapping for seedling and adult plant resistance to stripe rust in synthetic hexaploid wheat. *PLoS One* **9**:e105593.
- Zeng, Q., Wu, J., Liu, S., Chen, X., Yuan, F., Su, P., Wang, Q., Huang, S., Mu, J., Han, D., et al.** (2019a). Genome-wide mapping for stripe rust resistance loci in common wheat cultivar Qinnong 142. *Plant Dis.* **103**:439–447.
- Zeng, Q., Wu, J., Liu, S., Huang, S., Wang, Q., Mu, J., Yu, S., Han, D., and Kang, Z.** (2019b). A major QTL co-localized on chromosome 6BL and its epistatic interaction for enhanced wheat stripe rust resistance. *Theor. Appl. Genet.* **132**:1409–1424.
- Zheng, X., Qiao, L., Liu, Y., Wei, N., Zhao, J., Wu, B., Yang, B., Wang, J., and Zheng, J.** (2021). Genome-wide association study of grain number in common wheat from Shanxi under different water regimes. *Front. Plant Sci.* **12**:806295.
- Zhou, X.L., Han, D.J., Chen, X.M., Mu, J.M., Xue, W.B., Zeng, Q.D., Wang, Q.L., Huang, L.L., and Kang, Z.S.** (2015). QTL mapping of adult-plant resistance to stripe rust in wheat line P9897. *Euphytica* **205**:243–253.
- Zhu, T., Wang, L., Rimbert, H., Rodriguez, J.C., Deal, K.R., De Oliveira, R., Choulet, F., Keeble Gagnère, G., Tibbits, J., Rogers, J., et al.** (2021). Optical maps refine the bread wheat *Triticum aestivum* cv. Chinese spring genome assembly. *Plant J.* **107**:303–314.
- Zhu, Z., Cao, Q., Han, D., Wu, J., Wu, L., Tong, J., Xu, X., Yan, J., Zhang, Y., Xu, K., et al.** (2023). Molecular characterization and validation of adult-plant stripe rust resistance gene *Yr86* in Chinese wheat cultivar Zhongmai 895. *Theor. Appl. Genet.* **136**:142.